CFTR deficiency causes PMCA4 dysfunction, intracellular Ca^{2+} elevation and promotes epithelial cell damage in alcoholic pancreatitis and hepatitis

Tamara Madácsy

Ph.D. Thesis

Supervisor: Dr. József Maléth

Doctoral School of Theoretical Medicine
Department of Internal Medicine
University of Szeged
Szeged, Hungary

2022

List of pulications related to this thesis:

I. **Tamara Madacsy**, Árpád Varga, Noémi Papp, Bálint Tél, Petra Pallagi, Viktória Szabó, Aletta Kiss, Júlia Fanczal, Zoltan Rakonczay Jr, László Tiszlavicz, Zsolt Rázga, Meike Hohwieler, Alexander Kleger, Mike Gray, Péter Hegyi, József Maléth; Impaired Regulation of PMCA Activity by Defective CFTR Expression Promotes Epithelial Cell Damage in Alcoholic Pancreatitis and Hepatitis. **CELLULAR AND MOLECULAR LIFE SCIENCES** (2022) D1 **IF: 9.261**

List of publications not related to this thesis:

I. Pallagi, Petra; Görög, Marietta *; Papp, Noémi; **Madácsy, Tamara**; Varga, Árpád; Crul, Tim; Szabó, Viktória; Molnár, Melinda; Dudás, Krisztina; Grassalkovich, Anna et al. Bile acid- and ethanol-mediated activation of Orai1 damages pancreatic ductal secretion in acute pancreatitis. **JOURNAL OF PHYSIOLOGY-LONDON** (2022) D1 DOI: 10.1113/JP282203 **IF: 5,182**

II. Balla, Z; Kormanyos, ES; Kui, B; Balint, ER; Für, G; Orján, ME; Ivanyi, B; Vecsei, L; Fulop, F; Varga, G, **Madacsy, T,** et al. Kynurenic acid and its analogue SZR-72 ameliorate the severity of experimental acute necrotizing pancreatitis. **FRONTIERS IN IMMUNOLOGY**: Q1 DOI: 10.3389/fimmu.2021.702764 **IF: 7,561**

III. Breunig, Markus; Merkle, Jessica; Wagner, Martin; Melzer, Michael K; Barth, Thomas F E; Engleitner, Thomas; Krumm, Johannes; Wiedenmann, Sandra; Cohrs, Christian M; Perkhofer, Lukas, **Madacsy, Tamara** et al. Modeling plasticity and dysplasia of pancreatic ductal organoids derived from human pluripotent stem cells. **CELL STEM CELL** (2021) D1 DOI: 10.1016/j.stem.2021.03.005 **IF: 24,633**

IV. Déri, Szilvia; Borbás, János; Hartai, Teodóra; Hategan, Lidia; Csányi, Beáta; Visnyovszki, Ádám; **Madácsy, Tamara**; Maléth, József; Hegedűs, Zoltán; Nagy, István et al. Impaired cytoplasmic domain interactions cause co-assembly defect and loss of function in the p.Glu293Lys KNCJ2 variant isolated from an Andersen-Tawil Syndrome patient. **CARDIOVASCULAR RESEARCH** (2021: D1 DOI: 10.1093/cvr/cvaa249 **IF: 10,787**

V. Kata Judit, Szántó; **Tamara, Madácsy**; Diána, Kata; Tamás, Ferenci; Mariann, Rutka; Anita, Bálint; Renáta, Bor; Anna, Fábián; Ágnes, Milassin; Boldizsár, Jójárt et al. Advances in the optimisation of therapeutic drug monitoring using serum, tissue and faecal anti-tumour necrosis factor concentration in patients with inflammatory bowel disease treated with TNF-α antagonists. **EXPERT OPINION ON BIOLOGICAL THERAPY** (2021) Q1 DOI: 10.1080/14712598.2021.1890712 **IF: 4,388**

VI. Bálint, Anita; Farkas, Klaudia; Méhi, Orsolya; Kintses, Bálint; Vásárhelyi, Bálint Márk; Ari, Eszter; Pál, Csaba; **Madácsy, Tamara**; Maléth, József; Szántó, Kata Judit et al. Functional Anatomical Changes in Ulcerative Colitis Patients Determine Their Gut Microbiota Composition and Consequently the Possible Treatment Outcome. **PHARMACEUTICALS** (2020) D1 DOI: 10.3390/ph13110346 **IF: 5,863**

VII. Fanczal, Júlia; Pallagi, Petra *; Görög, Marietta; Diszházi, Gyula; Almássy, János; **Madácsy, Tamara**; Varga, Árpád; Csernay-Biró, Péter; Katona, Xénia; Tóth, Emese et al. TRPM2-mediated extracellular Ca^{2+} entry promotes acinar cell necrosis in biliary acute pancreatitis. **JOURNAL OF PHYSIOLOGY-LONDON** (2020) D1 DOI: 10.1113/JP279047 **IF: 5,182**

VIII. Molnár, Réka; **Madácsy, Tamara**; Varga, Árpád; Németh, Margit; Katona, Xénia; Görög, Marietta; Molnár, Brigitta; Fanczal, Júlia; Rakonczay, Zoltán; Hegyi, Péter et al. Mouse

pancreatic ductal organoid culture as a relevant model to study exocrine pancreatic ion secretion **LABORATORY INVESTIGATION** (2020) Q1 DOI: 10.1038/s41374-019-0300-3 **IF: 5,662**

IX. Pallagi, Petra; **Madácsy, Tamara***; Varga, Árpád; Maléth, József Intracellular Ca^{2+} Signalling in the Pathogenesis of Acute Pancreatitis: Recent Advances and Translational Perspectives. **INTERNATIONAL JOURNAL OF MOLECULAR SCIENCES** (2020) D1 DOI: 10.3390/ijms21114005 **IF: 5,924**

X. 11. Bakondi, Edina; Singh, Salam Bhopen *; Hajnády, Zoltán; Nagy-Pénzes, Máté; Regdon, Zsolt; Kovács, Katalin; Hegedűs, Csaba; **Madácsy, Tamara**; Maléth, József; Hegyi, Péter et al. Spilanthol Inhibits Inflammatory Transcription Factors and iNOS Expression in Macrophages and Exerts Anti-inflammatory Effects in Dermatitis and Pancreatitis. **INTERNATIONAL JOURNAL OF MOLECULAR SCIENCES** (2019) D1 DOI: 10.3390/ijms20174308 **IF: 4,556**

XI. **Madacsy, Tamara***; Pallagi, Petra *; Maleth, Jozsef Cystic Fibrosis of the Pancreas: The Role of CFTR Channel in the Regulation of Intracellular Ca^{2+} Signaling and Mitochondrial Function in the Exocrine Pancreas. **FRONTIERS IN PHYSIOLOGY** (2018): Q2 DOI: 10.3389/fphys.2018.01585 **IF: 3,201**

XII. Szentesi, A; Toth, E; Balint, E; Fanczal, J; **Madacsy, T**; Laczko, D; Ignath, I; Balazs, A; Pallagi, P et al. Analysis of Research Activity in Gastroenterology: Pancreatitis Is in Real Danger. **PLOS ONE** (2016) Q1 DOI: 10.1371/journal.pone.0165244 **IF: 2,806**

XIII. **Madácsy, T;** Maléth, J New findings in the pathogenesis of acute pancreatitis. CENTRAL EUROPEAN JOURNAL OF GASTROENTEROLOGY AND HEPATOLOGY / GASZTROENTEROLÓGIAI ÉS HEPATOLÓGIAI (2015)

XIV. Maleth, J *; **Madacsy, T** *; Pallagi, P; Balazs, A; Venglovecz, V; Rakonczay, Z Jr; Hegyi, P Pancreatic epithelial fluid and bicarbonate secretion is significantly elevated in the absence of peripheral serotonin. **GUT** (2015) D1 DOI: 10.1136/gutjnl-2015-309776 **IF: 14,921**

XV. Bereczki, Zsolt; **Madácsy, Tamara**; Király, Kitty; Sóskuti, Kornél, Paja, László Szarmata sebészi trepanációk a Kárpát-medencében **ANTHROPOLOGIAI KÖZLEMÉNYEK** 61 pp. 25-32. ,8p.(2020) DOI: 10.20330/AnthropKozl.2020.61.25

Number of full publications: 16 (5 first author)

Cummulative IF: 109.927

Table of contents

List of abbreviations

AH- alcoholic hepatitis;

AP- acute pancreatitis;

CF- cystic fibrosis;

CFLD- CF-associated liver disease;

CFTR- cystic fibrosis transmembrane conductance regulator;

CPA- cyclopiazonic-acid;

DMSO- dimethyl sulfoxide;

EPI- exocrine pancreatic insufficiency;

ER- endoplasmic reticulum;

EtOH- ethanol;

FAEE- fatty acid ethyl ester;

HPO- human pancreatic organoids;

IP3R- Inositol triphosphate receptor;

iPSC- induced pluripotent stem cells,

ITGB1- integrin beta-1;

KRT19- Cytokeratin 19;

MLO- mouse liver organoids;

MPO- mouse pancreatic organoids;

PA- palmitic acid;

PMCA- plasma membrane calcium pump;

POA- palmitoleic acid;

SERCA- sarco/endoplasmic reticulum Ca^{2+}-ATPase;

SOCE- store operated calcium entry;

STIM1- Stromal interaction molecule 1;

$\Delta\Psi m$ - mitochondrial membrane potetial;

Introduction

The exocrine pancreas and the pancreatic ductal epithelial cells

The pancreas in a retroperitoneal organ consisting of two main parts, the endocrine and an exocrine pancreas. 80% of the pancreas consists of acinar cells while about only 4-5% are ductal cells, 4% blood vessels and about 8% endocrine cells, yet ductal cells contribute largely to the secreted daily amount. Pancreatic jus an alkaline rich fluid which varies between 2-2,5 l daily [1]. Acinar cells secrete isotonic, mostly plasma like fluid, rich in proteins (enzymes and precursors), while the ducts determine the final electrolyte composition by reabsorbing Cl^- and secreting HCO_3^- into the lumen [1,2]. Pancreatic ductal secretion has a high importance in the normal homeostasis of the pancreas. According to our current knowledge pancreatic ducts are not only responsible for the mechanical structure of the pancreas but they also have the important role of secreting fluid and bicarbonate into the lumen [3]. The maximum HCO_3^- concentration of the juice secreted is up to 140mM [4]. Distal HCO_3^- secretion largely depends on the activity of CFTR, while the proximal ductal HCO_3^- secretion (ducts close to the acinar cells) is mainly mediated by the SLC26A6 Cl^-- HCO_3^- exchanger [5,6]. The mechanism of ductal HCO_3^- transport requires both HCO_3^- influx across the basolateral membrane and HCO_3^- exit through the luminal membrane [1]. In a healthy pancreas the digestive enzymes produced by the acini are washed out by this HCO_3^- rich fluid into the duodenum where it neutralizes the pH **(Figure 1.)**. Previously Pallagi et al. demonstrated that the autoactivation of trypsinogen is a pH dependent process, and has elevated activity in acidic environment, which means that HCO_3^- prevents the early autoactivation of trypsinogen, thus preventing the development of acute pancreatitis [7]. Our group have previously shown the importance of the ductal fluid secretion in experiments on mice which have shown that the ductal fluid secretion has a direct correlation with the severity of acute pancreatitis [8].

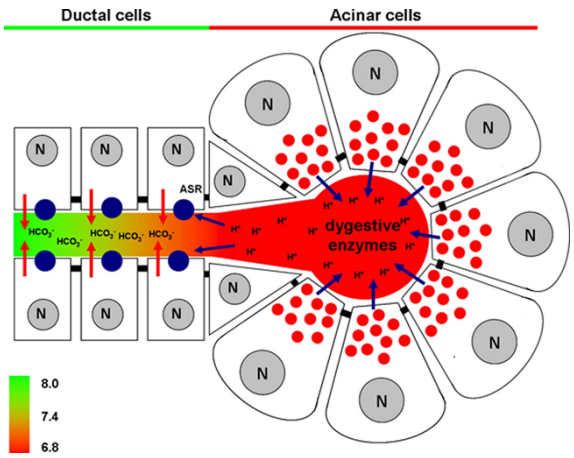

Figure 1. Changes of luminal pH in the pancreas during secretion. Under physiological conditions acinar cells secrete digestive enzymes and protons, the latter of which acidify the acinar lumen. In contrast, ductal cells secrete bicarbonate which will elevate the intraluminal pH. Our hypothesis is that protons may stimulate the ductal bicarbonate secretion via acid sensing receptors (ASR), which can elevate the pH in the ductal lumen setting the luminal pH to 8.0. (N, nucleus). *Hegyi et al 2011* [9]

Role of cystic fibrosis transmembrane conductance regulator in epithelial cell physiology

CFTR was discovered in 1989 as the faulty protein behind cystic fibrosis [10,11]. Since its discovery, it has become one of the most extensively studied proteins and serves as a model to understand the function of the proteins with a similar structure [12]. CFTR is part of the ABC transporters superfamily. However, unlike most ABC transporters (that are membrane pumps for organic molecules transporting their substrates against the electrochemical gradient using energy generated from ATP hydrolysis), it functions as a Cl^- permeable anion channel. Apart from being a chloride channel CFTR has a very important role in regulating the apical membrane conductance pathways [13]. It consists of five domains, two transmembrane (TM), two cytoplasmic nucleotide-binding domains (NBD) and a regulatory (R) domain [14,15]. In non-stimulated cells NBD1 binds to an unphosphorylated R domain to prevent the interaction between NBD1 and NBD2, and thus the hydrolysis of ATP which is essential for the opening of the channel. During stimulation agonists that bind to adenylyl cyclase (AC) coupled receptors activate protein kinase A (PKA) and increase the intracellular cAMP. The active PKA phosphorylates the R domain resulting it to dissociate from NBD1 and allowing the interaction between NBD1 and NBD2. The released R domain can form connections between CFTR and other transporters and membrane proteins, such as SLC26A6 Cl^-/HCO_3^- exchanger [16,17]. The SLC26A6 connects via STAS domain leading to a simultaneous activation of the two membrane proteins [1].

CFTR was found in several functionally different organs and tissues including lung, salivary glands, oesophagus, stomach, biliary tract, pancreas, intestine, kidney, heart, vas deferens and sweat ducts and play a fundamental role in secretory processes [18] **(Figure 2.)**. Evidence also shows that the channel also transports HCO_3^- and it has a central role in ductal secretion, through the strictly regulated interaction of SLC26A6 and CFTR [19,20]. In epithelial cells anion transport through the CFTR represents the rate-limiting step for secretion which controls the transepithelial fluid secretion and hydration of the epithelial luminal surfaces [21]. The luminal Cl^- concentration is also another important factor that coordinates the permeability of CFTR [1]. In the proximal part of the pancreatic ducts (where the Cl^- concentration is higher than 30 mM) the CFTR provides the extracellular substrate for the SLC26A6, while in the distal part the intracellular and the luminal Cl^- concentration drops, thus the Cl^-/HCO_3^- exchange of SLC26A6 becomes inadequate. This low intracellular Cl^- activates the With-No-Lysine (WNK) related proline/alanine-rich kinase (SPAK) pathway, turning CFTR permeable for HCO_3^- [22].

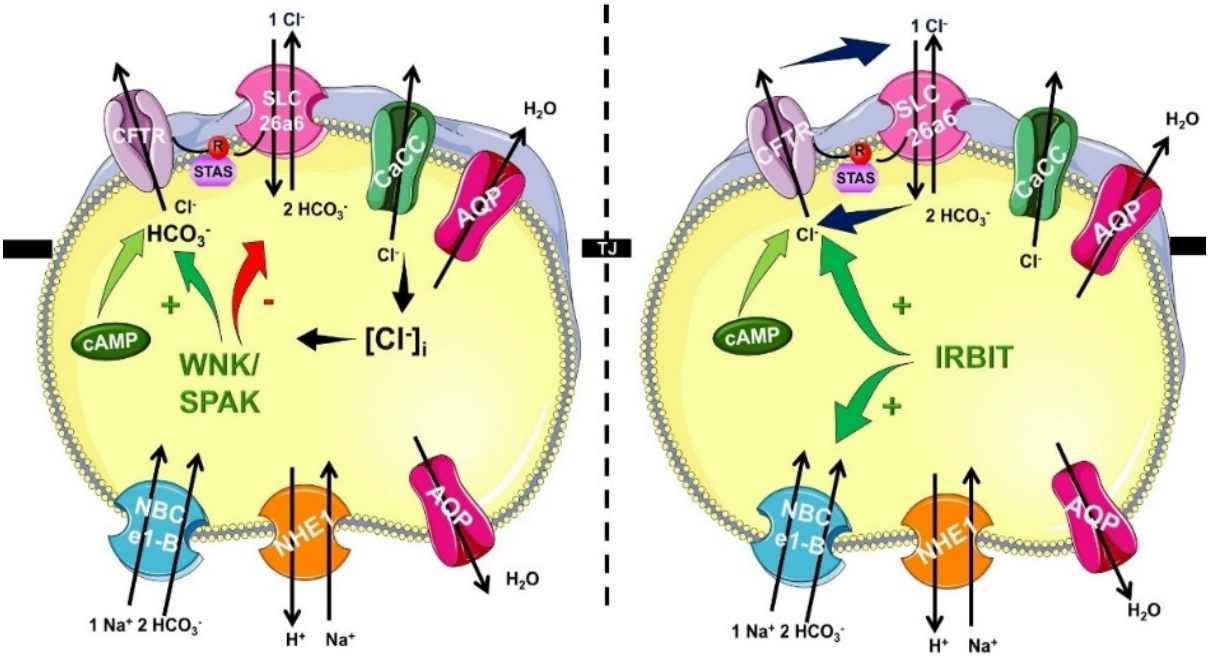

Figure 2: Mechanism of pancreatic ductal HCO_3^- secretion Pancreatic ductal cells secrete HCO_3^- rich isotonic fluid because of a complex interplay by several transport proteins. HCO_3^- is accumulated across the basolateral membrane Na^+/HCO_3^- cotransporter NBCe1-B. Via the luminal membrane HCO_3^- is secreted by SLC26A6 and likely A3 Cl^-/HCO_3^- exchangers and cystic fibrosis transmembrane conductance regulator (CFTR) Cl^- channel. The CFTR R domain and the STAS domain of the SLC26 Cl^-/HCO_3^- exchangers interact increasing the overall open probability of CFTR.- Madácsy et al 2018 [12]

The role of damaged CFTR function and expression in exocrine pancreatic damage

The genetic mutations of the CFTR lead to different pancreatic phenotypes [23]. Most CF patients develop pancreatic insufficiency over time. This is more likely to happen if both CFTR alleles carry the mutation which results in loss of function. CFTR mutations can be both severe and mild which can develop idiopathic recurrent acute or chronic pancreatitis. Heterozygous carriers of CFTR mutations increase the risk of developing pancreatitis [24]. Sharer and Cohn had published their discovery in 1998 that CFTR variants are overrepresented in CP [25,26] many follow-up studies have proven their findings. It has been demonstrated earlier that CF patients have lower secretion rate joined with high protein concentration which can participate in the damage of the pancreatic ductal lumen [21]. The changes begin to form *in utero*. After birth the obstruction of small ducts leads to large duct obstruction as well. Since some proteins originating from the pancreas get released into the bloodstream a few months after birth, this serves as an early screening method for CF. This process causes severe inflammatory changes like ductal obstruction, acinar destruction, and fibrosis.

Besides the genetic mutations, other toxins may cause the damage of CFTR, which can affect the exocrine pancreatic tissue homeostasis. This has been highlighted by Maléth et al. in 2015 when they found that the alcohol-induced functional inhibition and expressional defect of CFTR Cl^- channel in pancreatic ductal epithelial cells (PDEC) has increased the severity of acute pancreatitis [27]. Patients with alcoholic acute pancreatitis (AP) had lower levels of CFTR then the control group. They have demonstrated that ethanol and fatty acids dose-dependently reduce CFTR expression and activity in PDEC and also inhibit the fluid and HCO_3^- secretion [27]. CFTR inhibition by ethanol and fatty acids was associated with the increase of intracellular Ca^{2+} levels and cAMP and ATP depletion. Supplementation with ATP almost completely prevented CFTR inhibition [28]. The connection between CFTR and acute pancreatitis has been presumed. Di Magno et al. has shown that CFTR knockout mice develop more severe acute pancreatitis upon cerulein hyperstimulation with elevated pancreatic oedema, neutrophil infiltration and increased mRNA expression of inflammatory mediators [29]. The authors have focused on the acinar cell function though CFTR is expressed in the pancreatic ducts, and this increased severity is most likely caused by the compromised ductal fluid and HCO_3^- secretion. [21] The channel's role in AP was further investigated by examining the scaffolding protein Na^+/H^+ exchanger regulatory factor-1 (NHERF-1) in ductal function by Pallagi et al. The deletion of NHERF-1 reduced the expression of CFTR on the apical membrane of the PDEC and reduced fluid and HCO_3^-secretion [8]. In chronic pancreatitis (CP) CFTR dysfunction has been observed due to its mislocalized protein expression in pancreatic ductal cells [27]. The decreased expression is likely the cause of impaired ductal function, [30] and it leads to diminished fluid and HCO_3^- secretion due to the depleted activity of the $Cl^-/2$ HCO_3^- exchanger and the CFTR which leads to a lowered intraluminal pH, decreased washout of the digestive enzymes and a protein rich ductal fluid [31].

The possible role of CFTR in the development of alcoholic hepatitis

Annually 3 million deaths result from excessive alcohol consumption worldwide representing 5.3% of all deaths, whereas in the age group 20–39 years approximately 13.5 % of the total deaths are attributed to alcohol [32]. Among alcohol-related disorders the diseases of the liver and pancreas emerge due to their therapeutic challenges and socioeconomic burden [32,33]. Alcoholic hepatitis (AH) is a potentially lethal complication of alcoholic liver disease, which has been attributed to hepatocellular damage in the past [36]. Recent studies showed that cholestatic liver injury can be involved in the pathogenesis of AH, moreover, impaired

secretion by cholangiocytes, or cholestasis, results in a worse outcome [37]. Takeuchi et al. highlighted that integrin beta-1 (ITGB1)-mediated binding of neutrophils to cholangiocytes in AH results in the development of cholestasis [38]. It is well-established that cholangiocyte secretion largely depends on the proper function of the apically expressed CFTR [39]. Therefore considering that the alcohol-mediated effect on CFTR expression has been observed in other organs, such as the sweat glands [35], it is tempting to speculate that impaired CFTR expression might contribute to AH-related cholestasis.

Regulatory points between CFTR and Ca^{2+} signalling

CFTR is a traditionally a cAPM activated channel, though several studies found interactions between the Ca^{2+} and the cAMP signalling[44]. In the pancreas adenylyl cyclases induce the increase of cAMP levels and the activation of PKA [45]. The phosphorylation of CFTR by PKA in the apical membrane of ductal epithelial cells enhances chloride conductance into the lumen. These changes will increase the driving force of the sodium-bicarbonate co-transporter (NBC), will lead to the entry of HCO_3^- on the basolateral side and this bicarbonate will be secreted through the apical chloride-bicarbonate exchanger (CBE) and CFTR. The increase of the cAMP level will inhibit the sodium-hydrogen exchanger (NHE) and this might occur through direct interaction with CFTR. These signalling hubs are more than likely to be mediated by microdomains. It was already suggested in 2005 by Wang at al. that soluble adenylyl cyclase is involved in the regulation of CFTR in the context of human airway epithelium [46]. Supporting this idea in 2010 Namkung et al. have reported the regulation of CFTR by Adenylyl Cyclase I [47]. They have shown in primary cultures of human bronchial epithelial cells how CFTR is mediated through the Ca^{2+} activation of AC1 and cAMP/PKA signalling. They have also found the colocalization of the two in the apical membrane of the cells. The authors suggest that this AC1-CFTR association is responsible for the crosstalk of Ca^{2+}/cAMP signalling.

The Ca^{2+} activation of the CFTR channel have been suggested before in relation of HCO_3^- secretion of the pancreatic ductal epithelial cells by Namkung et al. They have tested CAPAN-1 cells and CFPAC-1 cells, and reported that calcium signals activate the Cl^- dependent HCO_3^- transport of CFTR [47]. Seidler et al. stated in 1997, that a functional CFTR protein is required for cAMP-; cGMP and calcium dependent bicarbonate secretion in the intestine of the mouse [48]. They show 75-100% reduction of Carbachol-stimulated HCO_3^- secretion in CFTR KO mice. More evidence on the effect of calcium on CFTR have been

demonstrated by Rasmussen et al. when they have shown how the localisation and surface density of CFTR appeared to be Ca^{2+} sensitive [49]. Even more links were suggested between the CFTR-Ca^{2+} synergism before, another possible link is the inositol 1,4,5-triphosphate (IP3) receptor-binding protein, Irbit [50]. Park et al. in 2014 found that Irbit mediates the activation of CFTR and SLC26a6 [50]. Their activation was shown to be mediated by Ca^{2+} and cAMP in pancreatic and salivary ducts as well as cultured HeLa cells.

Though conventionally CFTR is a cAMP regulated channel the paradigm of its interactions with other signalling pathways needs to be renewed. There are several studies suggesting the interaction of CFTR with the Ca^{2+} signalling pathway other then Ca^{2+} regulated adenylyl cyclases. Further evidence of the synergism of the cAMP and the Ca^{2+} signalling pathways were provided in 2017 when Bozoky et al. showed the regulation of CFTR by challenging the calmodulin binding site of the CFTR channel and reporting a calmodulin related activation of CFTR, independent of PKA [51]. Their experiments have shown CFTR and calmodulin colocalisation on the apical membrane of the cells. Patch-clamp experiments show calmodulin, when loaded with calcium to trigger an open probability, suggesting that it binds to CFTR. They have found that increased intracellular calcium can activate both WT and F508del CFTR. They have also characterised the Calmodulin-CFTR-R-region interactions and noted that the strength of the interaction is mediated by both calcium and the phosphorylation of the R-region. In 2011 Balghi et al have found elevated Ca^{2+} entry in CFBE cells due to enhanced Orai1 insertion into the plasma membrane in cystic fibrosis [52]. The elevated Ca^{2+} entry as a result can contribute to the inflammation known in cystic fibrosis. And very importantly they also suggest that Orai1 is part of a PM complex and potentially even a microdomain around CFTR: Some studies also link PMCA to this calcium hub near CFTR [52]. Recently Philippe et al have shown that both SERCA and PMCA can contribute to the deregulation of the Ca^{2+} homeostasis in cystic fibrosis. The SERCA pump's activity increased abnormally while PMCA function decreased in CF-cells. They have also demonstrated elevated mitochondrial Ca^{2+} uptake in CF cells compared to healthy, control bronchial epithelial cells [53]. They showed in the human bronchial CF epithelial cell line (CFBE) that ER retention increases in F508del mutation while PMCA function decreases compared to the ones treated with VX809 (a F508-del-CFTR mutation folding corrector). They have also shown on CFBE and 16HBE cells the interaction of SERCA2b and CFTR; and the interaction of PMCA and CFTR.

Altered mitochondrial function in epithelial cells in the lack of CFTR

The sustained elevation of intracellular Ca^{2+} is known to lead to mitochondrial Ca^{2+} overload. As early as 1972 Antonowicz et al have found alteration of the lysosomal α-glucosidase but did not find any faulty in the three mitochondrial enzymes tested. Few years later Shapiro et al reported an abnormal mitochondrial phenomenon in CF, they also found alterations of the calcium uptake and oxygen consumption in isolated mitochondria effected by CF. Their group have also shown abnormal pH of mitochondrial Complex1 and the dysfunction of energy expenditure in cystic fibrosis [54,55]. These same authors have also found that the mitochondria's increased Ca^{2+} uptake is associated with its altered respiratory system. Despite these early findings, after CFTR was cloned and proven to be a chloride channel, all the previous findings on the hypothesis of cytosolic, mitochondrial or lysosomal alteration in cystic fibrosis were scorned [11,55]. As the retention of F508del-CFTR can cause endoplasmic reticulum (ER) stress it can lead to disrupted Ca^{2+} signalling and cell death through mitochondrial damage [56]. The first publication strictly regarding CF and Ca^{2+} signalling was by Dennell et al. in 1961, where they found evidence of reparative fibrosis and altered calcium signalling [57]. Bloomfield et al. have reported elevated Ca^{2+} levels, altered parotid gland secretions and the hypersecretion of zymogen granules in CF patients. More recently Antigny et al in 2009 have shown that the mitochondrial network is fragmented, mitochondrial membrane potential ($\Delta\Psi_m$) is depolarised and Ca^{2+} uptake is reduced in CF mitochondria compared to control cells not effected by CF [58]. Antigny et al have also found in 2008 in F508del mutation when CFTR was rescued by miglustat or low temperature in human CF-KM4 cells Ca^{2+} mobilization decreased compared to uncorrected cells [56]. Their experiments with $CFTR_{inh}$-172 showed that simply inhibiting the function of CFTR, that it's the presence, not the function that is required to correct the Ca^{2+} mobilization in CF cells

The lack of functional CFTR alters epithelial cell fate

Under physiological conditions mitochondria are responsible for buffering released Ca^{2+} , on the other hand under pathophysiological conditions, the cell might lose control of the Ca^{2+} signalling and this can lead to mitochondrial Ca^{2+} overload and potential cell death[59,60]. For example, it is well known in the pathophysiology of acute pancreatitis how different toxic factors- such as bile acids, ethanol and its metabolites can be directly toxic to mitochondria. Depending on the damage type, the mitochondria can induce two different types of cell death. Apoptosis, being the controlled cell death, involving cell blebbing, shrinkage, nuclear fragmentation, chromatin condensation and chromosomal DNA fragmentation is ATP

dependent. One of the first events of apoptosis is the release of cytochrome c from the inner membrane of the mitochondrial electron transport chain and eventually leading to the activation of caspases, the ultimate mediators of apoptosis. On the other hand, necrosis is mostly unregulated. This type of cell death include decreased ATP production, loss of mitochondrial membrane potential ($\Delta\Psi_m$), vacuolization, loss of plasma membrane integrity, mitochondrial swelling and the leakage of intracellular contents[61].

Most work reported increased apoptosis in CF [55]. However some studies suggest it's the result of recurrent bacterial infections [62,63], while others state that apoptosis in CF occurs primarily even without bacterial infections [64,65]. The alterations include enhanced ROS production, release of cytochrome c and mitochondrial depolarisation while also the activation of c-Jun N-terminal kinases (JNKs) [62]. Some studies also conclude that this increased apoptosis might be due to the decreased antioxidant protection system, and this may contribute to the inflammation in CF [64,65]. Rottner et al have also linked the NF-κB pathway to the start of apoptosis in CF [66]. In relation it has been suggested before that the correction of F508-del-CFTR mutation reduces NF-κB mediated IL8 activation, one of the major inflammatory cytokine in CF lung [67].

Aims

During the Ph.D. studies my aim was to investigate the impact of ethanol mediated CFTR damage on intracellular Ca^{2+} homeostasis in pancreatic ductal epithelial cells and cholangiocytes.

Specific aim 1.:

Previously it has been suggested by several papers that there is a delicate relationship between CFTR and the Ca^{2+} homeostasis of cells [53,58] Therefore we aimed to:

- characterize the Ca^{2+} homeostasis in ethanol treated and CFTR KO pancreatic ductal epithelial cells
- identify the molecular background of the altered Ca^{2+} signaling

Specific aim 2.:

Bozoky et al. have found that CFTR interacts with several other plasma membrane proteins via calmodulin mediated binding [68] . Therefore, we aimed to:

- investigate the role of the calmodulin mediated interactions of CFTR in ethanol mediated cell damage

Specific aim 3.:

Maléth et al. have published in 2015 the damaging effect of ethanol on CFTR in pancreatic ductal epithelial cells [35]. The secretory functions of cholangiocytes also CFTR-dependent, therefore we aimed to investigate:

- effect of ethanol on CFTR activity and expression and intracellular Ca^{2+} signaling in cholangiocytes
- analyze the impact of ethanol mediated CFTR damage on mitochondrial function and cell viability in pancreatic ductal cells and cholangiocytes and the severity of alcohol induced pancreatitis in mice.

Materials and methods

Cell lines

HEK-293 and HeLa cells (ATCC; Cat. No.: ATCC-CRL-3249 and ATCC-CCL-2, respectively) were grown in DMEM (5796) (Sigma Aldrich, Cat. No.: D6421) containing 10% fetal bovine serum (FBS) (Sigma-Aldrich, Cat. No.: F7524), 1% Kanamycin (ThermoFisher Scientific, Cat. No.: 15160047), 1% Penicillin-Streptomycin (ThermoFisher Scientific, Cat. No.: 15140122) and 1% GlutaMax supplement (ThermoFisher Scientific, Cat. No.: 35050061) [69]. CFPAC-1 cells were a generous gift of Michael Gray (School of Biomedical, Nutritional and Sport Sciences; Newcastle University) and were grown in Iscove's modified Dulbecco's medium (ThermoFisher Scientific, Cat. No.: 12440061) supplemented as described above. Transfection of CFPAC-1 cells with recombinant Sendai virus containing the human CFTR gene was performed as described previously [70].

Animals

Cftr KO mice were originally generated by Ratcliff et al. and were kind gift of Professor Ursula Seidler [71]. Wild type (WT) refers to WT littermates of the *Cftr* KO animals. The mice used in this study were 8-12 weeks old and weighed 20-25 grams, whereas guinea pigs were 4–8-week-old. The gender ratio was 1:1 for all groups. The animals were kept at constant room temperature of 22-24°C under a 12 h light–dark cycle with free access to food and water. Animals received VRF1(P) standard rodent food (Special Diets Services, Cat. No.: 801900), and standard bedding were purchased from Akronom (Akronomm JRS; REHOFIX MK2000 corn cob). Interventions were done during the light cycle and animals were not fasted before the experiments. Animals were used with adherence to the NIH guidelines and the EU directive 2010/63/EU for the protection of animals used for scientific purposes. The study was approved by the National Scientific Ethical Committee on Animal Experimentation under license number XXI. /2523/2018.

Isolation of pancreatic ductal fragments and acinar cells

Pancreatic ductal fragments were isolated as described earlier [72]. Briefly after terminal anaesthesia with pentobarbital (270mg/bwkg) the pancreas was surgically removed from the animals and placed into ice-cold DME/F12 (Sigma-Aldrich, Cat. No.: D6421). The pancreas was injected with 100 U/ml collagenase (Worthington, Cat. No.: LS005273), 0.1 mg/ml trypsin inhibitor (ThermoFisher Scientific, Cat. No.: 17075029), 1 mg/ml bovine serum albumin (Sigma Aldrich, Cat. No.: A8022), in DME/F12 and placed into a shaking water bath at 37 ºC for 30 min. Small intra-/interlobular ducts were identified and isolated under

stereomicroscope. For pancreatic acinar cell isolation, the tissue was injected with 200 units/ml type 4 collagenase (Worthington, Cat. No.: LS004186) in standard HEPES and placed into a shaking water bath at 37 °C for 30 min as described previously. The tube was vigorously shaken every 5 min. The supernatant was centrifuged for 2 min at 129 RCF and the pellet was resuspended in Media 199 (ThermoFisher Scientific, Cat. No.: 11150059) with 0.1% BSA.

Mouse and human organoid cultures

Human pancreatic tissue samples were collected from transplantation donors (Ethical approval No.: 37/2017-SZTE). Mouse pancreatic, mouse liver and human pancreatic tissue samples were placed in Splitting media (Table 1). The pancreatic tissue was cut into small pieces with Gillette blade and was incubated in Digestion Media (Table 2) at 37 ºC in a vertical shaker for approximately 30 min, depending on tissue density. Digestion of the tissue was verified by stereo microscopy every 5 min. Cells were collected by centrifugation in a 15 ml centrifuge tube (113 RCF 10 min 4 ºC). Collected cells were washed by Wash Media (Table 3) two times. The pellet was resuspended in Wash Media and Matrigel (Corning, Cat. No.: 354234) in a ratio of 1:5. Matrigel domes (10 µl) were placed in one well of a 24-well cell culture plate and after 10 min of solidification at 37 ºC, 500 µl Feeding Media (Table 4) were applied in each well containing a dome. Feeding media was changed every other day. Domes were pooled and collected by centrifugation (113 RCF 10 min 4ºC) for passaging during which Matrigel removal and cell separation were performed simultaneously by TrypLE™ Express Enzyme (Gibco, Cat. No.: 12605028) at 37 ºC for 15 min in a vertical shaker followed by a washing step. Cell plating in Matrigel was performed as described above. For generating adherent 2D culture organoids were digested to single cells by TrypLE™ Express and washed two times as described above. Cells were cultured in feeding media during which 6-well plates and cover glass were applied. Both the organoids and adherent cells were kept under general culturing conditions (37°C, 95% relative humidity and 5% CO_2). 100 mM ethanol (EtOH) and 200 µM palmitic acid (PA) were administered to organoids at 37 °C in a humidified atmosphere overnight, before experiments. Organoids were used for experiments between passage numbers 1-5. The composition of different media is listed in tables 1-4.

Table 1 – Splitting Media

Component	Manufacturer/Cat.No.	Final cc/volume
Advanced DMEM/F-12	Gibco, 12634-010	500 ml
1 M HEPES	Gibco, 15630080	5 ml (10 mM)
GlutaMax Supplement (100X)	Gibco, 35050061	5ml (1X)
Primocin (400X)	Invivogen, ant-pm-2	1,25 ml (1X)

Table 2- Digestion media

Component	Manufacturer/Cat.No.	Final cc/volume
Splitting media	-	20 ml
Collagenase IV.	Worthington, LS004188	1250 U/ml
Dispase	Sigma-Aldrich, D4693	0,5 U/ml
FBS	Gibco, 10500064	0,5 ml 2,5% v/v
Trypsin inhibitor	Sigma-Aldrich, T9128	1mg/ml

Table 3- Wash media

Component	Manufacturer/Cat.No.	Final cc/volume
Splitting media	-	-
FBS	Gibco, 10500064	2,5% v/v
Antibiotic-Antimycotic Solution (100X)	Gibco, 15240062	1X
Kanamycin Sulfate (100X)	Gibco, 15160047	1X
Voriconazole	TOCRIS, 3760/10	2 µg/ml

Table 4- Feeding media

Component	Manufacturer/Cat.No.	Final cc/volume
Splitting media	-	19 ml
L-WRN conditioned media	-	25 ml
A-83	TOCRIS, 2939	500 nM
mEGF	Gibco, PMG8041	50 ng/ml
hFGF10	Peprotech, 100-26	100 ng/ml
Gastrin I	TOCRIS, 3006	0.01 µM
N-acetylcytstein	Sigma-Aldrich, A9165	1.25 mM
Nicotinamide	Sigma-Aldrich, N0636	10 mM
B-27 Supplement (50X)	Gibco, 17504001	1ml (1X)
Y-27632 Rho-Kinase Inhibitor	TOCRIS, 1254	10.5 µM
Prostaglandin E2 (PGE2)	TOCRIS, 2296	1 µM
Antibiotic-Antimycotic Solution	Gibco, 15240062	1 % v/v
Kanamycin (100X)	Gibco, 15160047	1X
Voriconazole	TOCRIS, 3764	2 µg/ml

Generation of human CF-specific induced pluripotent stem cells

Reprogramming of keratinocytes isolated from plucked hair of a CF patient or a healthy donor was performed to generate CF-specific and control induced pluripotent stem cells as previously described [73]. The pluripotent state of the established iPS cell lines was validated by immunostaining of essential pluripotency markers including OCT4, NANOG and SSEA4, and by transcriptional profiling. DNA sequencing confirmed the patient specific CFTR gene alteration in the respective iPSCs. The CF patient harboured the compound heterozygous mutations p.F508del and p.L1258Ffs*7.

Constructs and transfection

HEK-293 cells were transfected with plasmids coding EGFP-hPMCA4b, mCherry-CFTR-3xHA and mCherry-CFTR-3xHA(S768A). Transfection was carried out using Lipofectamine2000 (Invitrogene, Cat. No.: 11668-019) as described earlier [69]. EGFP-hPMCA4b was ordered from Addgene (Plasmid #: 47589). CFTR-3xHA was a generous gift from Gergely Lukács (McGill University, Montreal, Canada) [74], which was then cloned into a mCherry vector. Calmodulin binding site on human CFTR was disrupted by introducing a point mutation at the position 768 using Q5 Site-Directed Mutagenesis Kit (New England Nanolabs, Cat. No.: E0554S) resulting in a switch from serine to alanine (Fwd: AAGGAGGCAG**G**CTGTCCTGA, Rev: CGTGCCTGAAGCGTGG) [43]. Anti-CFTR siRNA (ON-TARGETplus Mouse siRNA, SMARTpool mouse CFTR, Dharmacon, Cat. No.: L-042164-00-0005) and transfection control (siGlo Green transfection indicator, Dharmacon, Cat. No.: D-001630-01-05) were used for *Cftr* silencing. The ducts were transfected with 50 nM siCFTR or siGLO Green transfection indicator in Opti-MEM (Gibco, Cat. No.: 31985070) then left to incubate for 12 h and were used for immunofluorescent staining or *in vitro* Ca^{2+} measurements.

Fluorescent microscopy

Intracellular Ca^{2+} concentration ($[Ca^{2+}]_i$), Cl^- ion levels, or intracellular pH were measured as described earlier [72] by loading the cells with Fura-2-AM (ThermoFisher Scientific, Cat. No.: F1201), MQAE (ThermoFisher Scientific, Cat. No.: E3101) or with BCECF-AM (ThermoFisher Scientific, Cat. No.: B1170), respectively. Ducts, acini, or organoids were attached to poly-L-lysine-coated (Sigma Aldrich, Cat. No.: P4707-50ML) coverslips and mounted on an Olympus IX71 fluorescent microscope equipped with an MT-20 illumination system. Filter sets for BCECF, Fura-2 and MQAE were described previously [72]. The signal was captured by a Hamamatsu ORCA-ER CCD camera trough a 20X oil immersion objective

(Olympus; NA: 0.8) with a temporal resolution of 1 s. Changes of $\Delta\Psi_m$ was followed by 100 nM tetramethylrhodamine-methyl ester (TMRM) (ThermoFisher Scientific, Cat. No.: T668) using a Zeiss LSM880 confocal microscope (excitation: 543 nm; emission: 560-650nm).

Gene expression analysis

Total RNA was isolated from whole pancreatic tissue or from isolated ductal fragments [72]. The isolated RNA was reverse transcribed, and amplicons were detected by ABI PRISM 7000 using SybrGreen (Maxima SYBR Green/ROx qPCR MasterMix, ThermoFisher Scientific, Cat. No.: K0222). Beta-2 microglobulin (B2M) and Proteasome Subunit Beta 6 (PSMB6) were selected for reference genes. Relative gene expression analysis was performed by ΔΔCq technique. RNA-seq was performed as follows, RNA extraction was carried out on mouse and human pancreatic ductal organoids. After the pellet collection of organoids from Matrigel, RNA was extracted with Nucleospin RNA plus kit (Macherey-Nagel, Cat. No.: 740984.25) according to manufacturer's protocol. RNA sequencing was carried out by an Illumina NextSeq 500 instrument. Data analysis service was provided by DeltaBio200 Ltd. The pattern of gene expression was determined by TPM (transcript/million) values.

Immunfluorescent labelling

Isolated pancreatic ducts, or organoids were frozen in Shandon Cryomatrix (ThermoFisher Scientific, Cat. No.: 6769006) and were sectioned by a Leica cryostat into 7 μM slices [72,74]. Cell lines were grown on cover glass and fixed without sectioning. Sections were fixed in 4% paraformaldehyde (PFA) in phosphate-buffered saline (PBS) for 15 min then washed in 1x Tris-buffered saline (TBS) for 3 x 5 min. After the 1 passage, fully grown organoids were placed into Shandon Cryomatrix and frozen at -20 ˚C. The slides were kept at -20 °C until staining. Immunofluorescent staining was performed in a humidified chamber at room temperature. Sections were fixed in 4% PFA-PBS for 15 minutes then washed in 1x TBS (Tris-buffered saline) for 5 min, repeated 3 times. Antigen retrieval was performed in 0.001 M Sodium Citrate (Sigma Aldrich, Cat. No.: C8532) (pH 6.0) and 0.05% Tween 20 (Sigma Aldrich, Cat. No.: P1379) buffer by heating the solution between 93-98°C then we placed the slides into the preheated solution for 20-30 min. After cooling to room temperature in 1xTBS the sections were blocked with 0.1% goat serum (Sigma Aldrich, Cat. No.: G9023) and 5% BSA-TBS (bovine serum albumin in Tris Saline Buffer) for 1 h. After blocking, the primary antibody diluted 1:100 in 5% BSA-TBS was administered then left for overnight incubation on 4°C. The next day the slides were washed 3x5 minutes in 1xTBS, then secondary antibody was added 1:400 in 5% BSA-TBS and incubated for 3h at room temperature, protected from

light. After 3h the slides were washed 3x5 min with 1x TBS, then Hoechst 1:1000 in 5% BSA-TBS was added and left for 15 min to incubate then washed 3 times in 1x TBS when mounting medium was added. The slides were covered, then left to dry in a dark slidebox. After drying the slides, they were stored at 4°C until visualising with confocal microscopy (ZEISS LSM 880). Antibodies were used according to Table 5. Applied antibodies are listed in Tables 6.

Table 5- Primary antibodies used during experiments

Name	Source	Clonality	Cat. No.	Provider
anti-CFTR	rabbit	polyclonal	ACL-006	Alomone Labs
anti-PMCA1	rabbit	polyclonal	ACP-005	Alomone Labs
anti- PMCA4	rabbit	polyclonal	ACP-004	Alomone Labs
anti-CFTR	mouse	monoclonal	ab2784	Abcam
panPMCA	mouse	monoclonal	ab2825	Abcam
anti-cytochrome C	mouse	monoclonal	ab13575	Abcam
anti-Calmodulin	rabbit	monoclonal	ab45689	Abcam
anti-caspase9	rabbit	monclonal	ab202068	Abcam

Table 6. Secondary antibodies used during experiments.

Name	Cat. No.	Provider
Goat anti-Mouse IgG (H+L) Cross-Adsorbed Secondary Antibody, Alexa Fluor 488	A-11001	Invitrogen
Goat anti-Mouse IgG (H+L) Highly Cross-Adsorbed Secondary Antibody, Alexa Fluor 594	A-11032	Invitrogen
Goat anti-Rabbit IgG (H+L) Cross-Adsorbed Secondary Antibody, Alexa Fluor 568	A-110011	Invitrogen
Goat anti-Rabbit IgG (H+L) Highly Cross-Adsorbed Secondary Antibody, Alexa Fluor 488	A-11034	Invitrogen
Donkey anti-Mouse IgG (H+L) Highly Cross-Adsorbed Secondary Antibody, Alexa Fluor 647	A-31571	Invitrogen
Goat anti-Rabbit IgG (H+L) Cross-Adsorbed Secondary Antibody, Alexa Fluor 568	A-11011	Invitrogen

Line Profile and Colocalisation Analysis

Line profile analysis was carried out with ImageJ FiJi (NIH) software by Plot Profile analysis of converted confocal images. Grey value intensity of the lines is shown in pictures. Maximal grey value intensity was averaged from 3-6 individual evaluations. Mander's coefficient was calculated by ImageJ JACoP plugin. All data are expressed as means ± SEM.

DuolinkDuolink® Proximity Ligation Assay

For DuolinkDuolink® assay (Sigma Aldrich, Cat. No.: DUO92014, DUO82049, DUO92001, DUO92005) guinea pig pancreatic ductal fragments were used due to the primary antibody compatibilities. The pancreata of guinea pigs were surgically removed and washed in PBS and pancreatic ductal fragments were isolated as described above. After cryoprotection, ductal fragments were frozen and sectioned as described above. Duolink® assay was performed on a humidified chamber according to the manufacturer's protocol (Sigma-Aldrich). Sections were fixed in 4% PFA-PBS for 20 min then washed in TBS 3 times for 5 min. Antigen retrieval was performed as described earlier. After cooling to room temperature, the sections were blocked by the Duolink®-blocking solution, and we progressed with the Duolink® protocol according to Sigma-Aldrich. Briefly, primary antibodies for CFTR and PMCA4 were incubated overnight at 4 °C. The next morning PLA plus and minus probes were incubated with the slides at 37 °C for 1 hour. In the next step Duolink® Ligase was added for 30 min at 37 °C. After the ligation of the plus and minus probes, the Duolink® Polymerase was added in Duolink® Amplification buffer for 100 min at 37 °C. After washing the slides according to the protocol, the samples were mounted in Fluoromount (Sigma Aldrich, Cat. No.: F4680) mounting medium and visualised with a ZEISS LSM 880 confocal microscope equipped with a Plan-Apochromat 40x oil immersion objective (NA 1.4; Zeiss). Images were taken as Z-stacks as suggested by Sigma-Aldrich.

Immunohistochemistry

Paraffin-embedded, 3- to 4-µm-thick sections of surgically removed resection specimens and autopsy liver tissue samples were used for immunohistochemistry. Immunohistochemical labelling was performed with a Leica Bond-MAX Fully Automated IHC and ISH Staining System. Briefly, deparaffinization step was carried out with Bond Dewax Solution (Leica biosystems, Cat. No.: AR9222) at 72 °C. After washing with BondTM Wash Solution (Leica biosystems, Cat. No.: AR9590), epitope retrieval was carried out with Bond TM Epitope Retrieval Solution (Leica biosystems, Cat. No.: AR9640) 2 at 100 °C for 20 min at pH 9. After slides were washed with wash solution at 35 °C, peroxidase blocking was performed by Novocastra Peroxidase Block (Leica biosystems, Cat. No.: RE7101-CE) for 5 min. Primary CFTR antibody was diluted in BondTM primary antibody diluent (Leica biosystems, Cat. No.: AR9352) and incubated on samples for 20 min. For immunohistochemical labelling and visualisation, Bond Polymer Refine Detection (Leica biosystems, Cat. No.: DS9800) was applied for 8 min. Sections from human pancreas were used as positive controls.

Direct Stochastic Optical Reconstruction Microscopy (dSTORM)

HeLa cells grown on cover glass were co-transfected with EGFP-hPMCA4b, mCherry-CFTR-3xHA and mCherry-CFTR-3xHA(S768A) plasmids. Primary human pancreatic ductal cells were isolated from transplantation donors and were generated for dSTORM by digesting and plating human pancreatic ductal organoids on cover glass. HeLa cells were fixed with 4% PFA for 10 min and AGR was performed by 0.01% Triton-X-100 (Reanal, Cat. No.: 32190-1-99-33) for 10 min. Applied antibodies are listed in Supplementary Table 6. Adherent primary cell and sectioned organoids were fixed and retrieved by methanol (Sigma Aldrich, Cat. No.: 34860) for 10 min at -20 °C. After fixation with 4% PFA in PBS for 10 min, antigen retrieval was performed by 0.01% Triton-X-100 in PBS for 10 min. Aspecific binding sites were blocked by applying 10% BSA in PBS for 2 h at 37 °C. The following primary antibodies (1:100) were used during overnight incubation at 4 °C: anti-PMCA4, anti-CFTR. Samples were washed three times for 10 min with PBS. Fluorophore conjugated secondary antibodies were applied prior to another washing step (3 x 10 min). For dSTORM imaging, cover glasses were placed on cavity slides (Sigma Aldrich, Cat. No.: BR475505-50EA) filled with blinking buffer and sealed with two-component adhesive (Picodent, Cat. No.: 13 007 100). Blinking buffer contains 100 U glucose oxidase (Sigma Aldrich, Cat. No.: G2133-50KU), 2000 U catalase (Sigma Aldrich, Cat. No.: C100), 55.5 mM glucose (Sigma Aldrich, Cat. No.: G8270) and 100 mM cysteamine hydrochloride (Sigma Aldrich, Cat. No.: M6500) in 1 mL final volume with sterile PBS. Cover glasses were placed in blinking buffer and dSTORM images were captured by Nanoimager S (Oxford Nanoimaging ONI Ltd.). Organoids derived from human pancreatic tissue were cryosectioned as described above and placed on cover glasses (VWR, ECN 631-1583). Sectioned organoids were fixed and retrieved by methanol for 10 min at -20°C. Further steps of immunofluorescence labelling as well as the imaging process are the same as previously described. Cluster analysis of dSTORM images were evaluated by CODI (Oxford Nanoimaging ONI Ltd.).

Transmission Electron Microscopy

The pancreas of WT and CFTR KO mice were surgically removed on ice after being sacrificed. We cut the pancreas into approximately 2 mm x 2 mm pieces and placed it into fixative solution overnight at 4°C in 2% glutaraldehyde in PBS containing 2.25% dextran (20KD). After fixation, the cells were embedded in Embed 812 (EMS, USA) with routine transmission electron microscope (TEM) embedding protocol. After the semithin sections (1 μm), the thin (70 nm) sections were made for TEM examination. To estimate the volume

fraction of mitochondria in cells, micrographs of 18-30 cells were prepared in each case, on a TEM. The fractions of the TEM micrographs were automatically generated into 9 images using the module of Jeol 1400 plus. The original magnification of TEM micrographs (single or montage) was 12000X. The area of cells and mitochondria were measured by point counting. The area per test point for cells were 500nm x 500nm, and 50nm x50nm for mitochondria. Three locations per mitochondria were estimated separately (luminal, middle and basal). The luminal area was defined from the luminal side of the ductal cells, tangent of nucleus, parallel with the luminal surface of the cell. The middle was between the two tangents of nucleus, parallel with the luminal surface of the cell. The basal area was defined as opposite of the basal side of the cells.

Experimental alcohol-induced acute pancreatitis in mice

We induced acute pancreatitis via fatty acid ethyl ester (FAEE) in wild-type FVB/N mice according to Huang et al. [75] The animals received two intraperitoneal injections of ethanol (1.35 g/kg) and palmitoleic acid (POA; 150 mg/kg) at 1-h intervals. Prior to the ethanol-POA injections, the animals received 200 µl physiological saline solution injection intraperitoneally to prevent potential damaging effects and to protect the organs at the injection site. Control animals received one intraperitoneal injection of vehicle (25% DMSO, 75% sterile water) 90 min before the administration of either saline or ethanol/POA. Treated groups received one intraperitoneal dose of aurintricharboxylic acid (ATA) (Sigma Aldrich, Cat. No.: A36883) (5mg/kg) in vehicle (25% DMSO, 75% sterile water) 90 min before the injections of either saline or ethanol/POA [76]. Animals were sacrificed 24 h after the first ethanol/POA injection. The severity of pancreatitis was assessed on both paraffin embedded hematoxylin eosin stained 5 µm slices, and the measurement of serum amylase activity. Hematoxylin eosin-stained slides were scored by three independent individuals, blind for the experimental set up. Scoring was carried out by the following histological parameters: edema, leukocyte infiltration and acinar cell necrosis [77]. The serum amylase activity was measured by Alpha Amylase Assay kit (Diagnosticum, Cat. No.: 47462) based on the colorimetric kinetic method. Absorbance of the samples were measured at 405 nm with a CLARIOstar Plus (BMG Labtech).

Results

Absence of CFTR impairs the function of plasma membrane Ca^{2+} pump in pancreatic ductal epithelial cells

Our hypothesis was that the decreased CFTR expression caused by chronic ethanol per se is sufficient to disturb the Ca^{2+} homeostasis of the gastrointestinal epithelial cells. Previously, we established that acute exposure to ethanol releases Ca^{2+} from the ER and activates extracellular Ca^{2+} influx in pancreatic ductal cells [35]. To assess whether the decreased CFTR expression disturbs the intracellular Ca^{2+} homeostasis wild-type (WT) and *Cftr* KO mice pancreatic ducts were challenged with carbachol. The maximal Ca^{2+} release was not different between the two groups, the slope of the Ca^{2+} signal plateau phase – representing the Ca^{2+} extrusion from the cytosol– was significantly higher in *Cftr* KO ductal fragments compared to WT **(Figure 3.A.)**. Next, we utilized mouse pancreatic organoids (MPO) generated from WT and *Cftr* KO mice. WT organoids were treated with 100 mM ethanol (EtOH) and 200 μM palmitic acid (PA) for 12 h, control and *Cftr* KO MPOs received no treatment. Store operated Ca^{2+} influx was activated by re-addition of the extracellular Ca^{2+} after ER depletion (25 μM cyclopiazonic-acid (CPA) in Ca^{2+}-free media) **(Figure 3.B.)**. The basal intracellular Ca^{2+} concentrations were significantly higher in the EtOH-treated and *Cftr* KO organoids **(Figure 3.C.)**. As expected, the ER Ca^{2+} release in response to CPA was lower in the EtOH treated organoids and was not changed in *Cftr* KO organoids **(Figure 3.D.)**, whereas both EtOH treated and *Cftr* KO organoids showed a significantly decreased Ca^{2+} extrusion after removal of the extracellular Ca^{2+} **(Figure 3.E.)**.

The same phenomenon was observed in *Cftr* KO ducts **(Figure 4.A.)**. Next, to confirm that the observed difference in Ca^{2+} extrusion was specific to CFTR-expressing cells, we analysed Ca^{2+} signaling in pancreatic acinar cells, which lack CFTR in general [78] and did not detect difference in the carbachol response (maximal intracellular Ca^{2+} release or extrusion) between WT and *Cftr* KO mice acini **(Figure 4.B.)**. Moreover, functional inhibition of CFTR with 10 μM CFTR(inh)-172 –which significantly impaired CFTR activity **(Figure 4.C.)** [35]– had no effect on the carbachol-induced Ca^{2+} extrusion in WT ductal cells **(Figure 4.D.)**.

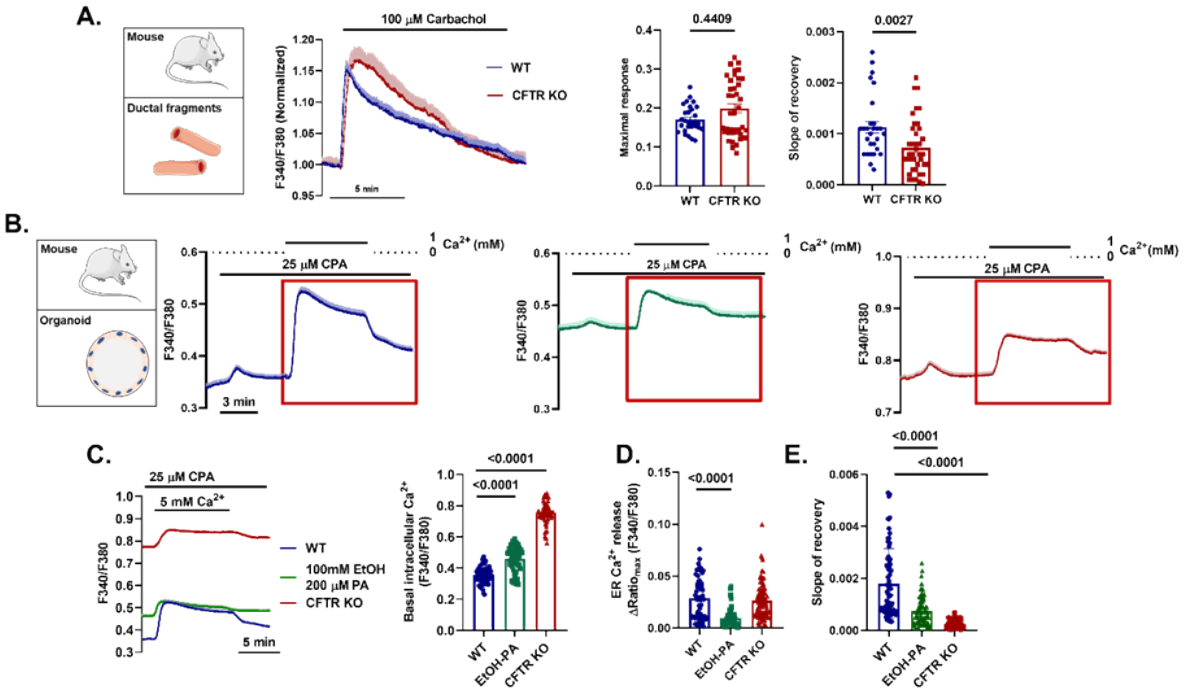

Figure 3. Lack of CFTR expression leads to impaired Ca^{2+} extrusion in mouse pancreatic ductal cells. A. Average traces of intracellular Ca^{2+} concentration ($[Ca^{2+}]_i$), maximal Ca^{2+} elevation, and the slope of recovery in wild type (WT) and *Cftr* KO pancreatic ductal fragments in response to 100 µM carbachol. **B.** Average $[Ca^{2+}]_i$ traces show the Ca^{2+} efflux after ER Ca^{2+} store depletion (red quadrant highlights the Ca^{2+} extrusion used to calculate the slope of recovery) of mouse pancreatic ductal organoids (**C**). The basal intracellular Ca^{2+} levels were elevated (**D**), whereas the Ca^{2+} extrusions (slope of recovery) were significantly reduced (**E**) both in EtOH/PA pre-treated and *Cftr* KO organoids

Next human pancreatic organoids (HPO) were treated with 100 mM EtOH and 200 µM PA overnight. Importantly, compared to untreated HPOs, Ca^{2+} extrusion was significantly decreased after pre-incubation with EtOH/PA **(Figure 5.A.)**.Correction of CFTR expression in CFPAC-1 cells [70]–derived from liver metastasis of a CF patient's pancreatic ductal adenocarcinoma–restored Ca^{2+} extrusion **(Figure 5.B.)**. In contrast, knockdown of CFTR expression in WT ductal fragments with siCFTR impaired Ca^{2+} extrusion compared to control **(Figure 5.C.)**.

Considering that both PMCA and Na^+/Ca^{2+} exchangers (NCX) can forward Ca^{2+} extrusion in non-excitable cells, we used the pan-NCX inhibitors SEA0400 and CB-DMB to assess the contribution of NCX to the process. None of these inhibitors had any effect on the slope of the decrease **(Figure 6.A-B.).** Recently, Partner of STIM1 (POST) –an adaptor protein linking STIM1 to other proteins– was shown to enhance the function of PMCA4 [79]. However, siSTIM1 treatment had no effect on the Ca^{2+} efflux in WT pancreatic ducts, suggesting that Stim1-POST is not involved in the regulation of PMCA in epithelial cells

(Figure 6.C.). Taken together, these results indicate that attenuation of CFTR expression - rather than the lack of activity- by ethanol treatment is sufficient to alter Ca^{2+} homeostasis through limiting PMCA activity.

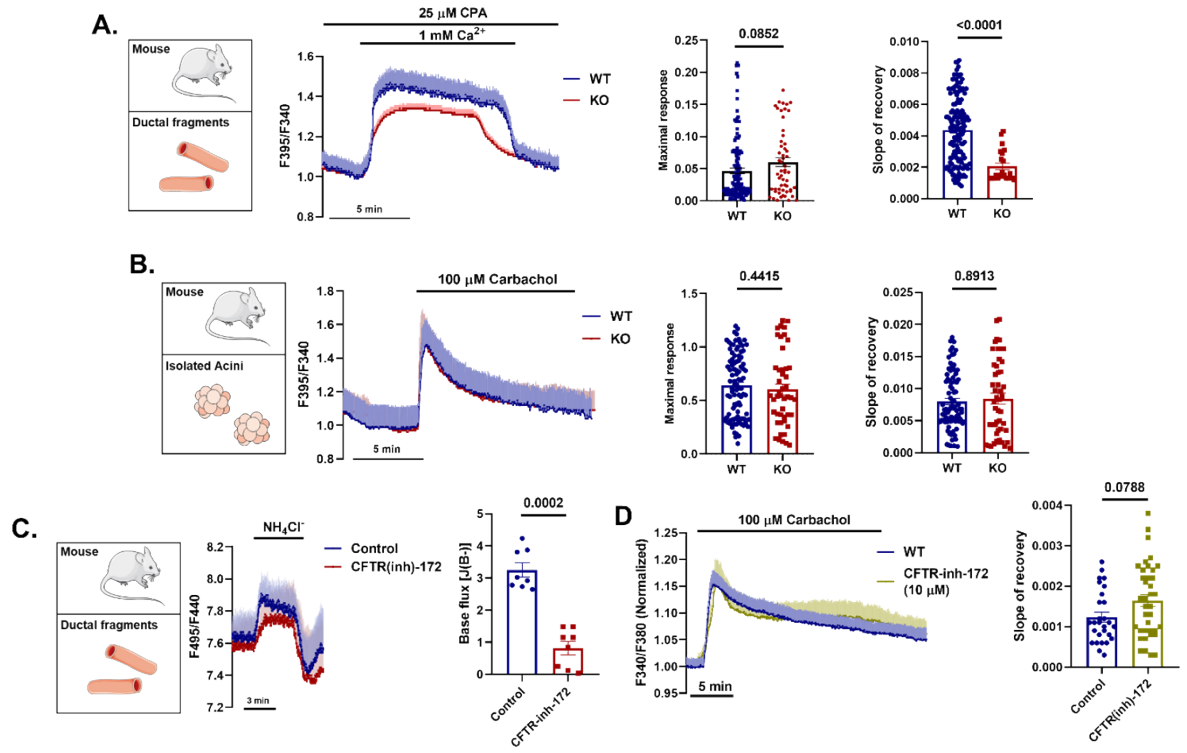

Figure 4. Lack of CFTR expression leads to impaired Ca^{2+} extrusion in mouse pancreatic ductal cells A. Average traces and bar chart shows that the Ca^{2+} release from the ER during 25 µM CPA treatment did not show significant difference among WT CFTR KO pancreatic ductal fragments, whereas the Ca^{2+} extrusion was significantly impaired. **B.** Average traces of the maximal Ca^{2+} elevation and the slope of recovery in WT and Cftr KO pancreatic acinar cells in response to 100 µM carbachol showed no difference. **C.** Average traces and bar charts demonstrating the effect of CFTR inhibition in isolated pancreatic ducts. The inhibition of CFTR significantly decreased the recovery from alkali load. n: 4-10 individual experiments **D.** Average traces of $[Ca^{2+}]i$ and the slope of recovery demonstrate that inhibition of CFTR function has no effect on the intracellular Ca^{2+} signaling.

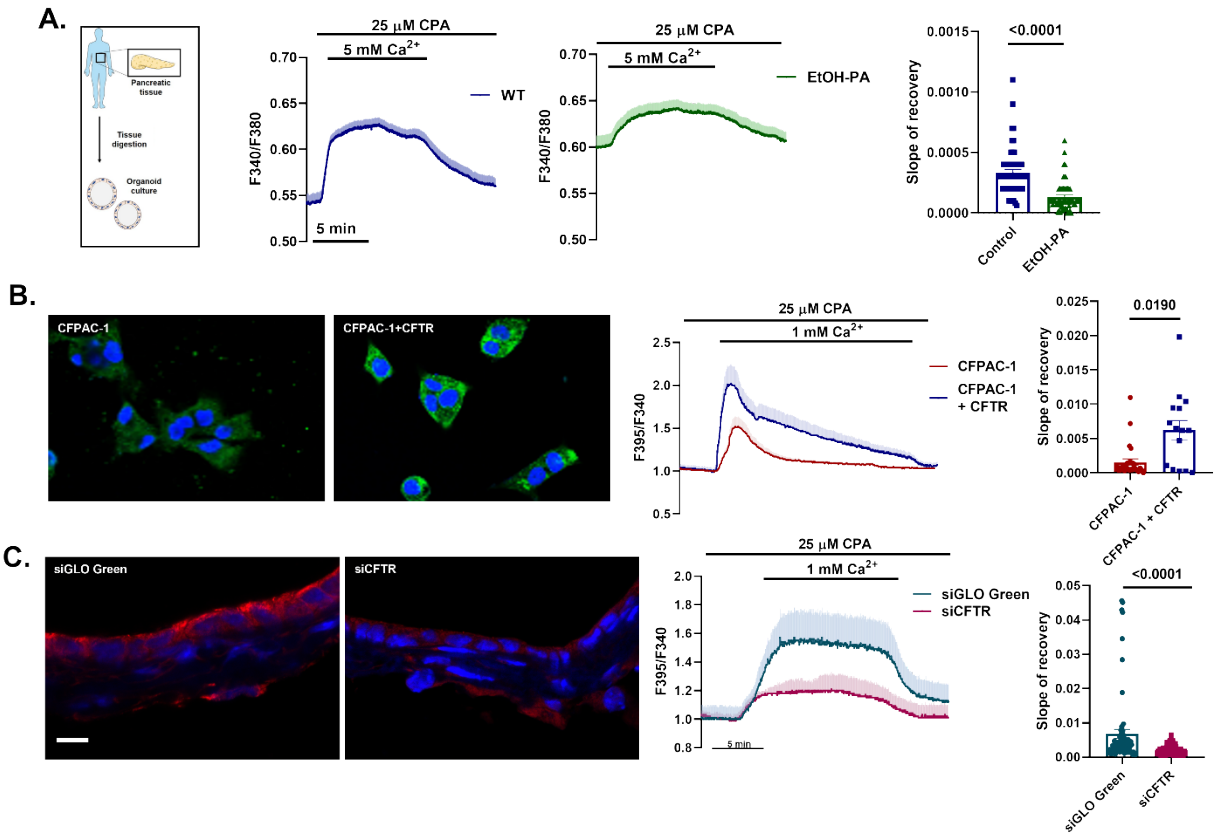

Figure 5. Lack of CFTR expression leads to impaired Ca^{2+} extrusion in mouse pancreatic ductal cells. A. Average traces and bar chart show that the Ca^{2+} extrusion was significantly decreased in EtOH/PA pre-treated human pancreatic organoids. **B.** Restoration of CFTR expression in CFPAC-1 human pancreatic ductal cell line CFPAC-1 with Sendai virus mediated gene delivery was confirmed by immunostaining. Average traces of intracellular Ca^{2+} concentration and bar chart of the slope of recovery highlight that the correction of CFTR expression also improved PMCA function. **C.** siRNA-mediated knockdown in isolated mouse ductal fragments markedly decreased apical CFTR distribution in mouse pancreatic ductal fragments. Average traces of intracellular Ca^{2+} concentration and bar chart of the slope of recovery demonstrate that the siCFTR treatment significantly decreased the PMCA4 function in mouse pancreatic ductal fragments

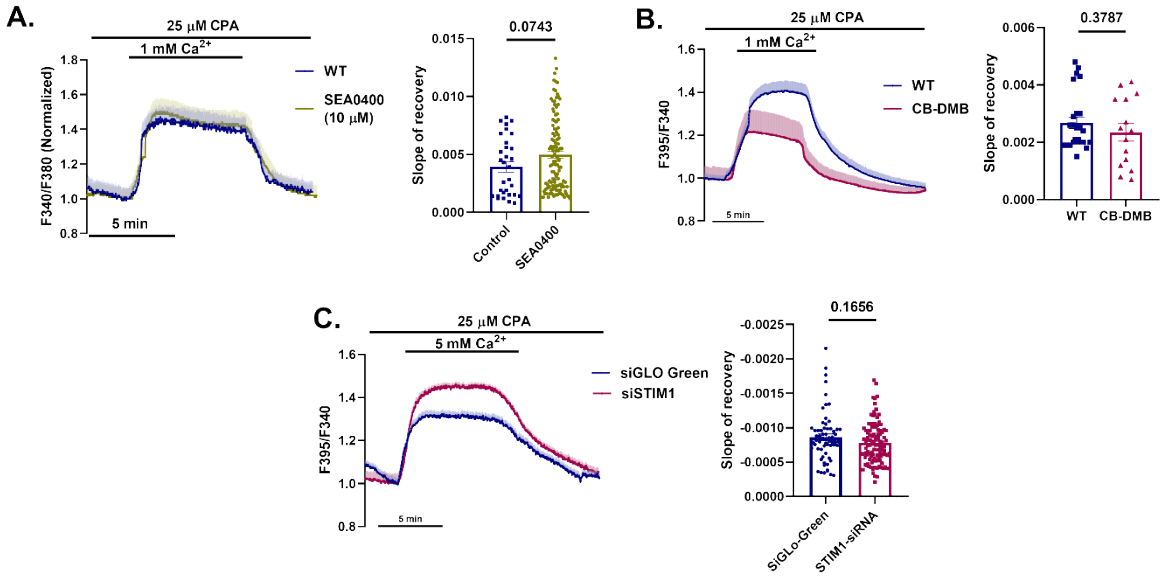

Figure 6. Inhibition of NCX and STIM1 does not affect the Ca^{2+} extrusion on PDEC A. Average traces and bar chart demonstrating that NCX inhibition with SEA0400 had no effect on the Ca^{2+} extrusion in pancreatic ductal cells. n=4-10. **B.** Average traces and bar charts demonstrating the inhibition of NCX with 10 μM CB-DMB had no effect on the Ca^{2+} extrusion in pancreatic ductal cells. **C.** Average traces and bar charts show the effect of STIM1 knock down on PMCA4 activity. Treatment of mouse pancreatic ductal fragments with siSTIM1 did not alter the PMCA4 function compared to SiGLO-Green treated ducts. Scale bars: 10 μm. n: 4-10 individual experiments.

Ethanol has no effect on the PMCA4 expression in pancreatic ductal cells

Currently, four mammalian PMCA genes have been identified which contribute to cytosolic Ca^{2+} extrusion [80]. Using whole transcriptome analysis, we revealed the expression of *Pmca1* and *Pmca4* in MPO and *PMCA1* and *PMCA4* in HPO samples, with highest levels of *Pmca1* in mouse and highest levels of *PMCA4* in humans **(Figure 7.A-B.)**. Of note, expression levels of *Pmca2* and *Pmca3* were below detection limit in all samples. RT-PCR followed by endpoint analysis confirmed the expression of *Pmca1* and *Pmca4* in whole pancreatic tissue as well as isolated mouse pancreatic ducts **(Figure 7.C.)**. Immunofluorescent staining of PMCA1 and PMCA4 in cross sections of mouse pancreatic ducts revealed the apical localization of PMCA4, whereas PMCA1 was evenly distributed over the apical and basolateral membranes **(Figure 7.D.)**. In addition, a strong co-localization of PMCA4 and CFTR at the apical membrane was observed (Mander's correlation coefficient:0.906, **(Figure 7.D.)**. To further confirm that CFTR has no effect on PMCA1 we incubated MPOs with the PMCA4 inhibitor aurintricarboxylic acid (ATA). Pre-incubation of MPOs for 30 min with 10 μM ATA *in vitro* significantly impaired the intracellular Ca^{2+} extrusion **(Figure 17.D.)**, however no difference was observed between pre-treated WT and CFTR KO organoids,

suggesting that PMCA1 function is not affected by the lack of CFTR **(Figure 7. E.)**. Similar moderate changes were observed in the Pmca1 expression in EtOH/PA-treated and *Cftr* KO MPOs (**Figure 7.F.**)

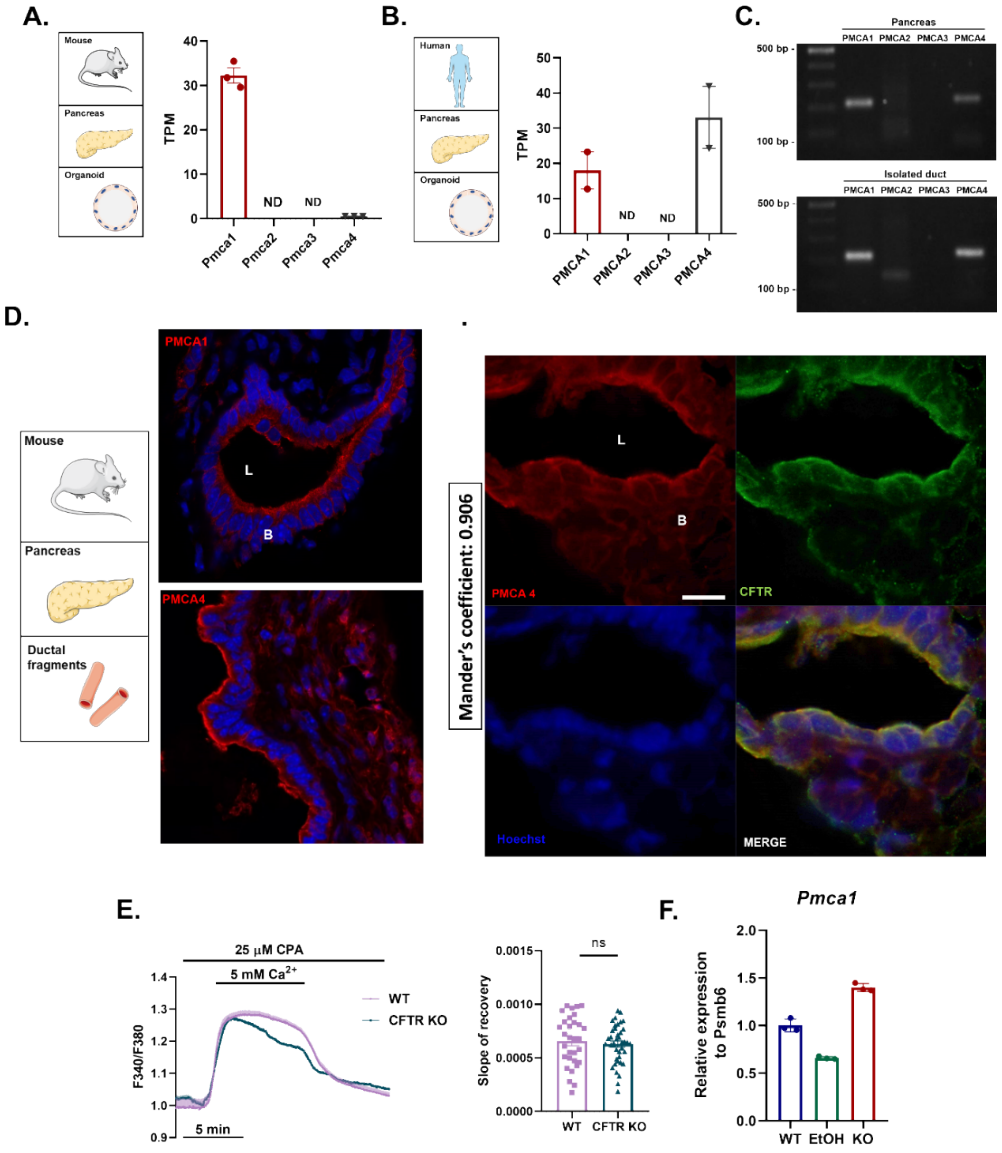

Figure 7 Ethanol has no effect on the PMCA4 expression of pancreatic ductal cells. Whole transcriptome analysis of **A.** mouse and **B.** human pancreatic organoids demonstrate the expression of *Pmca1* and *Pmca4* (given in TPM: transcripts per million). n=3 **C.** Endpoint RT-PCR analysis of PMCA isoforms in whole pancreas (left panel) and in isolated ducts (right panel). **D.** PMCA4 and CFTR colocalize at the apical membrane of pancreatic ductal epithelial cells in isolated mouse ductal fragments with a Mander's overlap coefficient of 0.906. Scale bars: 10 μm. B: basolateral side; L: lumen **D.** Average traces and bar charts demonstrating the effect of the PMCA4 inhibitor aurintricarboxylic acid (ATA) in mouse pancreatic organoids. ATA treatment impaired the intracellular Ca^{2+} extrusion, however no difference was observed between WT and CFTR KO organoids, suggesting that PMCA1 function is not affected by the lack of CFTR. **E-F.** Gene expression analysis of *Pmca1* relative to *Psmb6* showed no changes of *Pmca1* in mouse pancreatic organoid culture after EtOH-PA treatment, or in CFTR KO organoids

In intestinal stem cells, loss of CFTR expression results in alkaline pH_i deriving Wnt/β-catenin-mediated expression of different genes [81], which may affect the expression of PMCA4 in pancreatic ductal cells. To test this, the relative expression of *Pmca4* was compared with qRT-PCR in control, EtOH/PA-treated and *Cftr* KO MPOs. While control and EtOH/PA-treated WT MPO showed no significant alteration, *Pmca4* expression was moderately increased in *Cftr* KO ductal organoids compared to WT control suggesting that the difference of Ca^{2+} efflux is not due to reduced gene expression **(Figure 8.A.)**. Next, we wondered whether loss of CFTR due to EtOH treatment would alter the apical membrane-specific localisation of PMCA4. Whereas immunofluorescent microscopy revealed diminished CFTR levels at the apical membrane in EtOH/PA-treated and *Cftr* KO MPOs compared to untreated WT, PMCA4 retained its apical localisation in all samples **(Figure 8.B.)**. Subsequently, the presence of CFTR and PMCA4 on the apical plasma membrane of HPOs was confirmed by immunolabelling. Whereas overnight incubation of HPO with EtOH/PA resulted in a diminished, patchy apical expression pattern of CFTR, PMCA4 retained its apical membrane localisation **(Figure 8.C.)**. Notably, alcohol treatment resulted in a detectable cytosolic shift of PMCA4. These results suggest that the lack of CFTR at the apical membrane of pancreatic ductal cells diminishes the activity but not the expression or localization of PMCA4.

iPSC-derived organoids from cystic fibrosis patients recapitulate the alteration of PMCA function

Our results suggest that the diminished CFTR expression caused by genetic mutations in CF may also disturb Ca^{2+} extrusion of pancreatic ductal cells. Therefore, we assessed the relevance of our findings in human iPSC-derived pancreatic organoids generated from CF patients [73]. To establish CF-iPSC lines from donors affected by classical CF, lentiviral reprogramming of patient keratinocytes was used as previously described and performed stepwise *in vitro* differentiation to direct the iPSCs towards the pancreatic lineage followed by generation of exocrine pancreatic organoids in 3D-suspension culture **(Figure 9.A.)**. First, immunofluorescent analysis revealed that, while CFTR levels were absent in CF patient derived organoids, which was markedly restored by 12 h incubation with the CFTR-corrector VX-809 (10 μM), PMCA1 and PMCA4 expression was present in control- and CF patient-derived iPSC organoids **(Figure 9.B-C.)**. Then, Ca^{2+} removal after ER Ca^{2+} store depletion resulted in a significantly decreased Ca^{2+} extrusion in CF organoids compared to control,

further recapitulating our previous observation obtained in other model systems **(Figure 9.D.)**. Importantly, pre-treatment with 10 µM VX-809 for 12 h significantly improved Ca^{2+} extrusion indicating that CFTR corrector treatment can restore decreased PMCA activity and thus the Ca^{2+} extrusion in CF organoids.

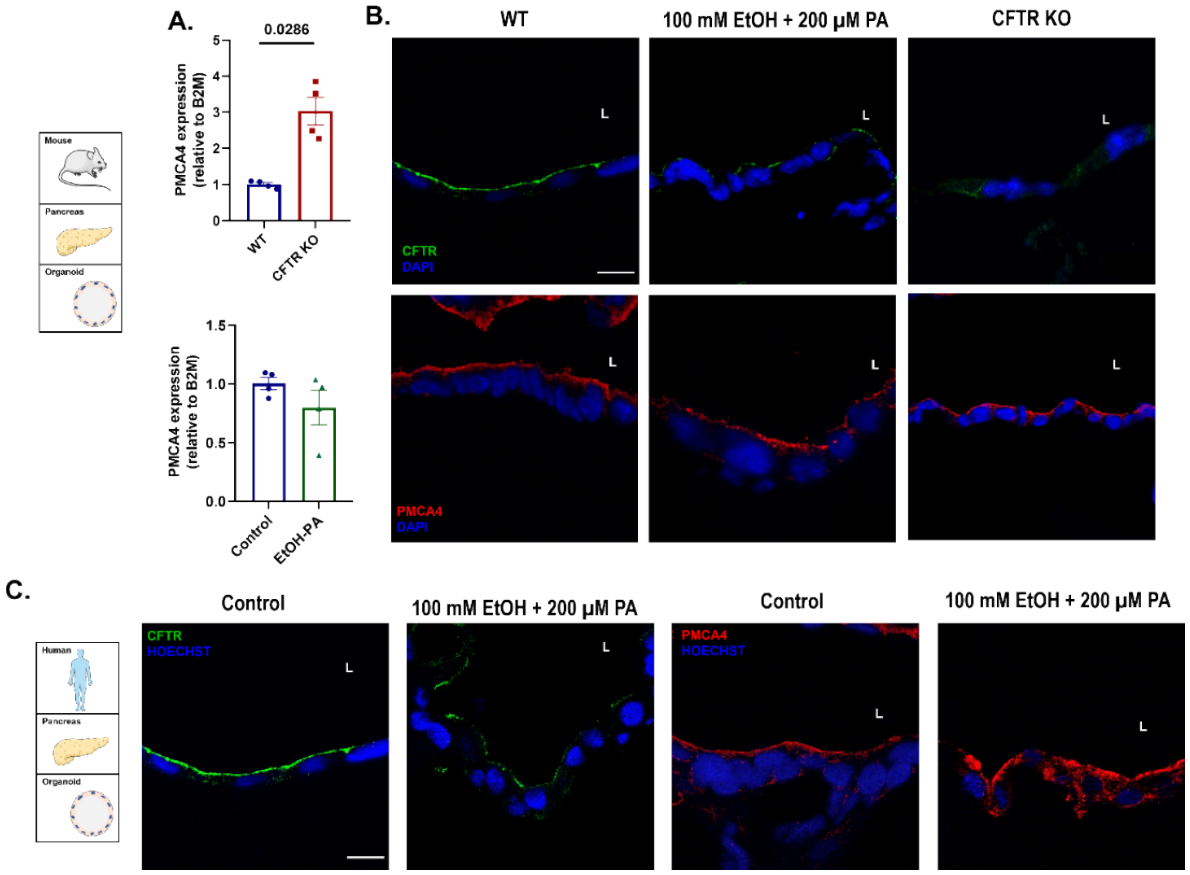

Figure 8. A. PMCA4 gene expression in MPOs relative to B2M. Pre-incubation with EtOH/PA had no effect whereas *Cftr* knockdown significantly increased the *Pmca4* expression.**B.** Localisation of PMCA1 and PMCA4 in mouse pancreatic organoids. **C.** Confocal images of mouse (F) and human (G) organoids show even, apical localisation of CFTR and PMCA4. This apical CFTR distribution was significantly impaired in *Cftr* KO and EtOH/PA pre-treated organoids. PMCA4 localization was not changed in MPO, whereas increased cytosolic staining was observed in HPOs. Scale bar=10µm n

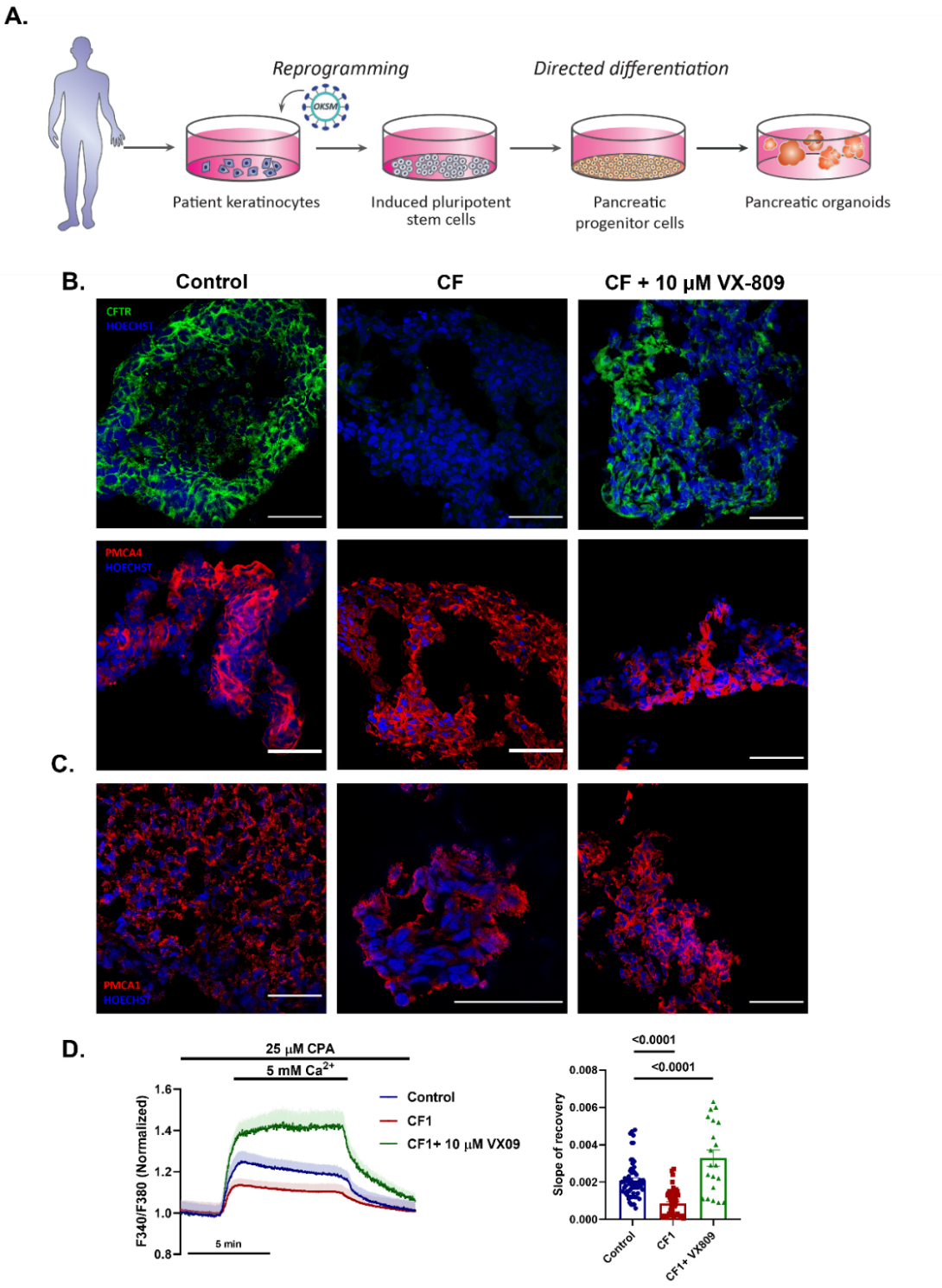

Figure 9. PMCA4 activity is decreased in cystic fibrosis human pancreatic organoids. A. Schematic outline of the generation of iPSC-derived pancreatic organoids from cystic fibrosis (CF). **B.** Confocal pictures confirm the presence of both CFTR and PMCA4 in control iPSC organoids, while CF organoids showed no staining for CFTR. 12 h incubation with 10 µM VX-809 restored CFTR expression in CF organoids. **C.** Average traces and bar charts highlight a significant decrease in the Ca^{2+} extrusion in CF organoids compared to control, which was markedly improved after VX809 treatment. Scale bars=20µm. n=4-10 individual experiments.

Ethanol reduces CFTR expression and PMCA activity in cholangiocytes

Although the cholangiocyte secretory function greatly depends on CFTR activity [39], alcohol-related changes in CFTR function or expression were never analysed in alcoholic hepatitis (AH). Immunohistochemistry on formalin-fixed paraffin-embedded liver samples revealed that the apical CFTR distribution in cholangiocytes was significantly impaired in patients with AH compared to controls **(Figure 10.A.)**. Next, we recapitulated this phenomenon *in vitro* in WT mouse-derived liver organoids (MLO) positive for the epithelial cell lineage marker KRT19 **(Figure 10.B.)**. CFTR showed a luminal membrane localisation in untreated MLOs, which was significantly decreased and shifted towards the cytosol in EtOH-treated MLOs without biologically relevant changes in *Cftr* gene expression levels **(Figure 10.C-D.)**.

Subsequent functional analysis of MLOs revealed a significantly impaired apical Cl^-/HCO_3^- exchange activity in EtOH/PA-treated MLOs compared to control **(Figure 11.A.)**. Also, whereas extracellular Cl^- removal resulted in CFTR-dependent increase in MQAE fluorescence –used as a marker of intracellular Cl^- [72]– in control MLOs, alcohol treatment resulted in a significant decrease of CFTR-dependent Cl^- extrusion **(Figure 11.B)**. Finally, Ca^{2+} measurements revealed significantly decreased PMCA activity in ethanol pre-incubated- as well as *Cftr* KO organoids compared to WT control, suggesting that decreased apical distribution of CFTR impairs PMCA function in cholangiocytes **(Figure 11.C.)**. Changes of *Pmca4* gene expression didn't achieve a biologically relevant level in MLOs **(Figure 11.D.).** Importantly, these results highlight that EtOH exposure alters CFTR localization and activity in cholangiocytes leading to decreased ion secretion and disturbed intracellular Ca^{2+} homeostasis.

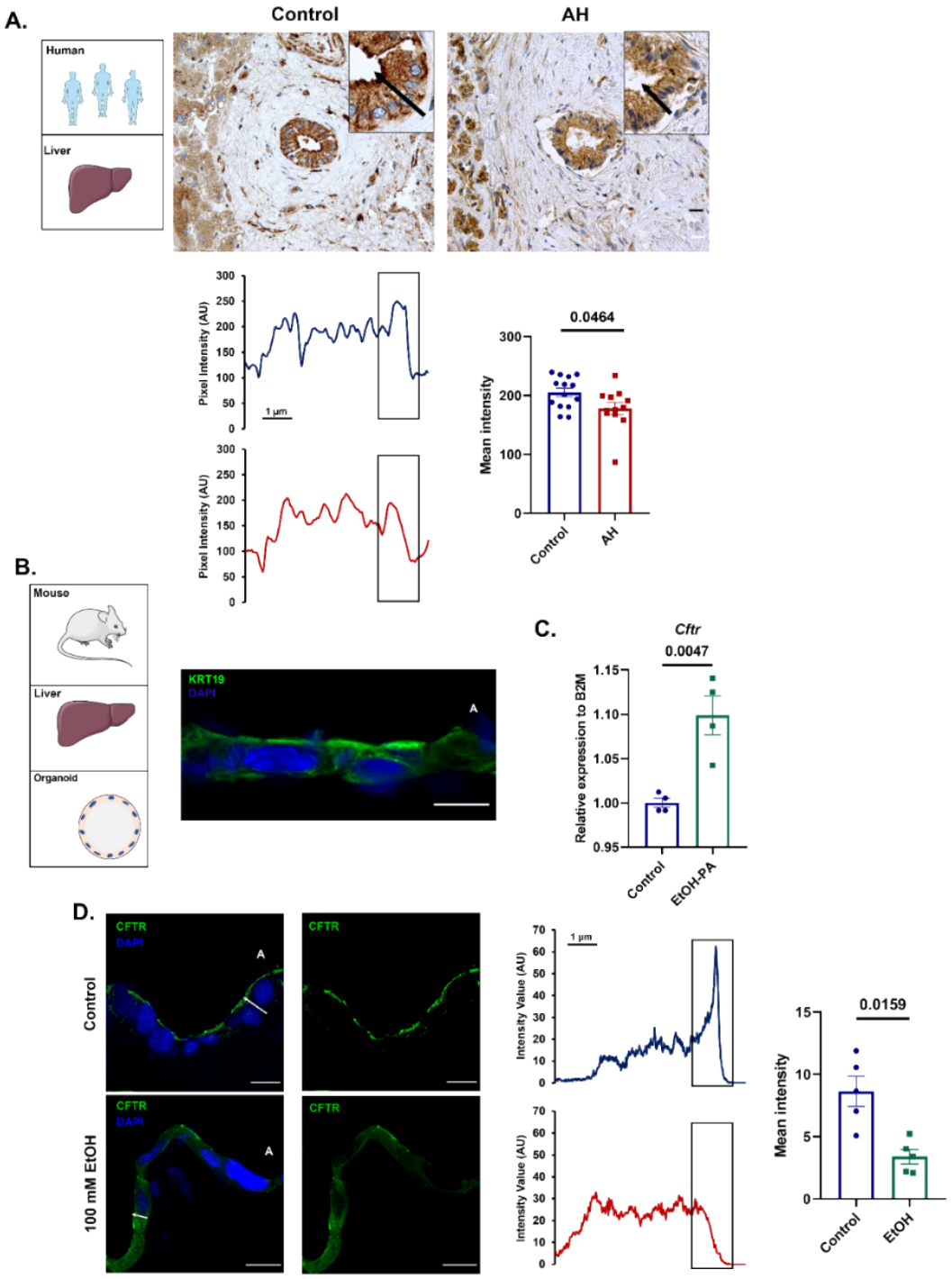

Figure 10. CFTR expression is impaired in cholangiocytes in alcoholic hepatitis. A. CFTR expression of human cholangiocytes (**A**) and mouse liver organoids (**D**). In control cholangiocytes and organoids CFTR is localized on the apical plasma membrane (black boxes). In patients with alcoholic hepatitis (AH) and EtOH/PA pre-treated organoids the apical distribution significantly decreased. Scale bar=10 µm. L: lumen. **B.** Immunofluorescent staining of Cytokeratin 19 confirms the epithelial fate of generated mouse liver organoid cultures, suggesting clean lineage of cholangiocytes. Scale bar: 10 µm. **C.** Gene expression analysis of *Cftr* relative to *b2m* showed minor elevation of *Cftr* in mouse liver organoid culture after EtOH-PA treatment.

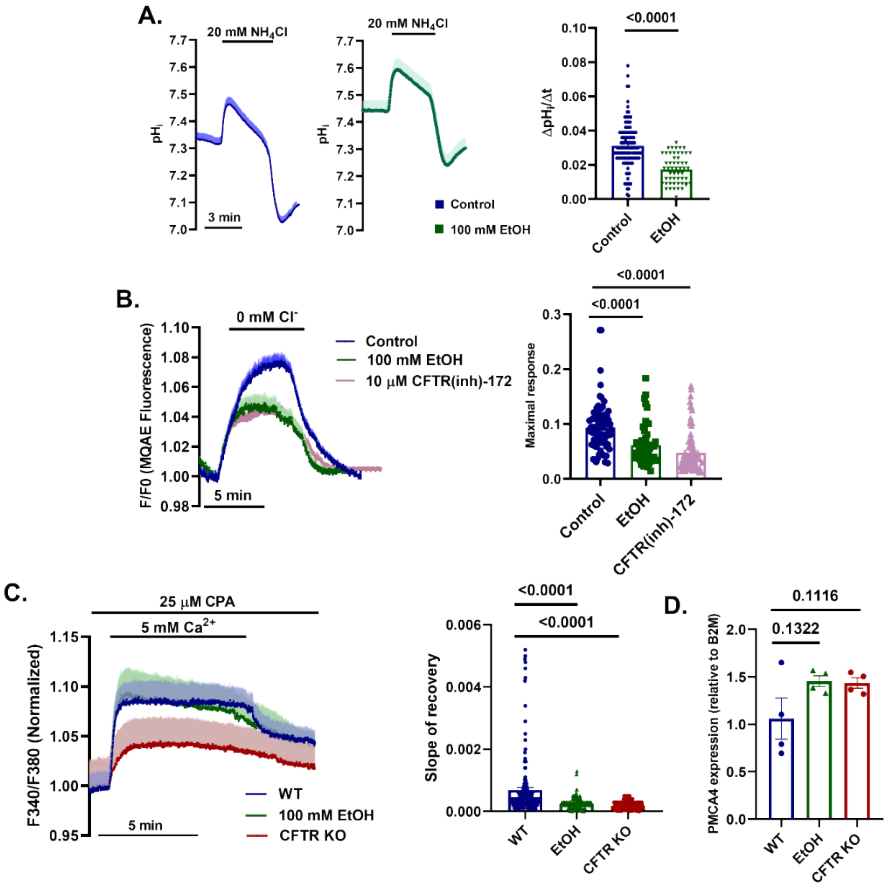

Figure 11. PMCA function is impaired in CFTR KO and EtOH/PA pre-treated liver organoids. A. Average traces show the regeneration from alkalosis in liver organoids after exposure to 20 mM NH_4Cl in HCO_3^-/CO_2-buffered solution. The base flux from alkali load represents the activity of the apical anion exchange, which was significantly decreased in EtOH/PA-treated liver organoids. **B.** Average MQAE traces show the CFTR-mediated Cl^- efflux after Cl^- withdrawal from the extracellular solution. The activity of CFTR was significantly reduced by overnight incubation of the liver organoids with EtOH/PA. **C.** Average traces and bar charts demonstrate that the Ca^{2+} extrusion is decreased in EtOH/PA pre-treated and in *Cftr* KO mouse liver organoids. **D** *PMCA4* gene expression was not changed in EtOH/PA pre-treated and in *Cftr* KO mouse liver organoids. n=4-6 individual experiments

PMCA4 interacts with CFTR at the apical membrane of pancreatic ductal epithelial cells

Our observations suggesting that proper PMCA4 activity requires a close connection with CFTR. Therefore, we performed Duolink proximity ligation assay (PLA) between endogenous PMCA and CFTR. Of note, to avoid non-specific antibody binding, guinea pig pancreatic ductal fragments were used, which recapitulated the colocalization of PMCA4 and CFTR **(Figure 12.A.)**. Duolink PLA suggested that PMCA4 and CFTR are in a proximity of <40 nm **(Figure 12.B.)**. Then, we used dSTORM to visualize this interaction at even higher

resolution. In HeLa cells co-transfected with plasmids encoding CFTR and PMCA4, we observed a perfect overlap (<20 nm) between the two proteins in the plasma membrane suggesting physical proximity **(Figure 12.C.)**.

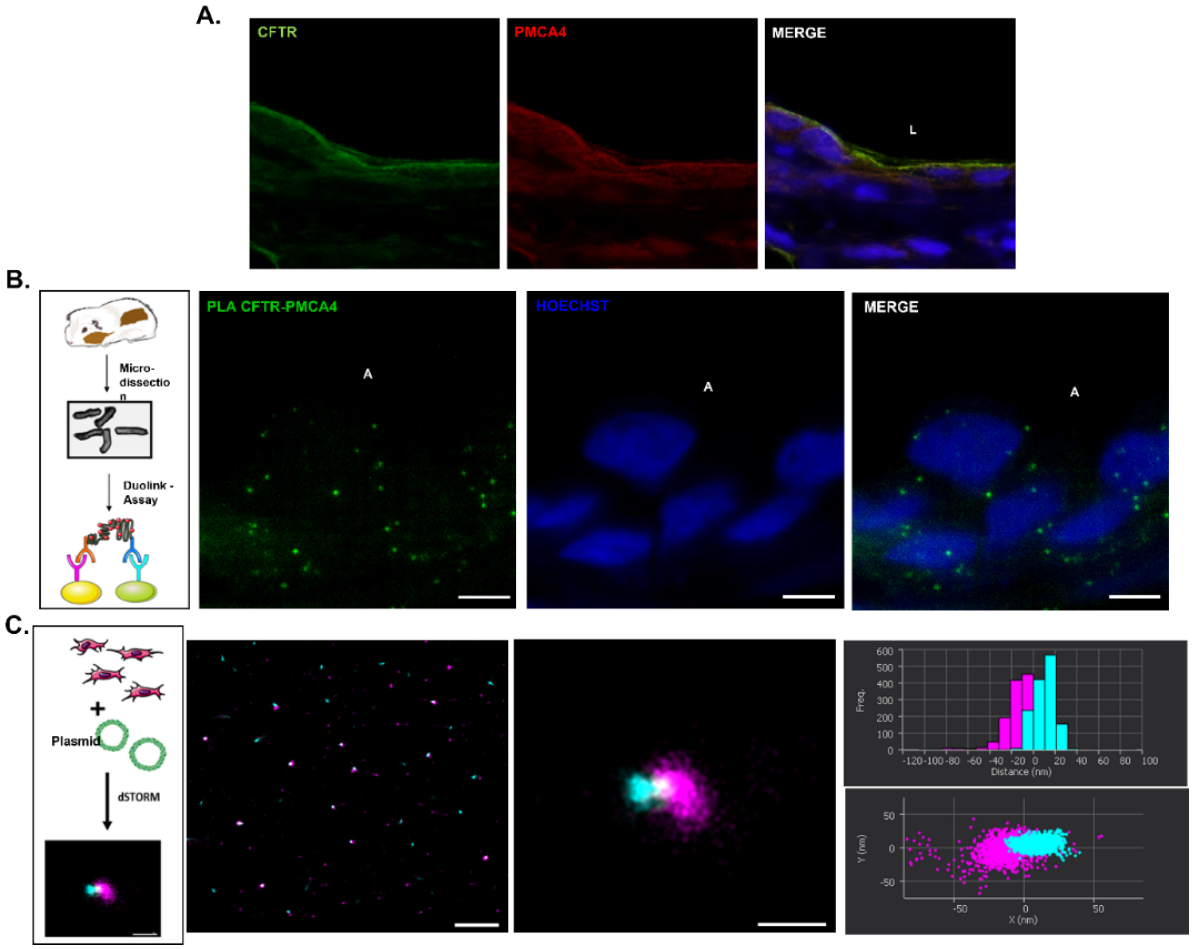

Figure 12. Interaction of PMCA4 with CFTR at the apical plasma membrane. A. Colocalization of CFTR and PMCA4 in isolated guinea pig pancreatic ducts. B: basolateral side; L: lumen. **B.** Endogenous PMCA and CFTR are in close proximity (<40 nm) as suggested by Duolink proximity ligation assay. (Merged image of 18 optical sections). Scale bar=10µm. **C.** dSTORM images of HeLa cells transfected with CFTR and PMCA4 revealed a perfect overlap (<20 nm) between the two proteins in the plasma membrane. Scale bars=1µm and 50nm, respectively.

Calmodulin binding by CFTR regulates PMCA4 activity in pancreatic ductal cells and in cholangiocytes

Next, we wanted to provide mechanistic insight into the regulation of PMCA4 activity by CFTR. The recently described alternative calmodulin binding of CFTR has been suggested to allow the regulation of other proteins [43]. Thus, we hypothesized that such type of calmodulin-CFTR interaction might subsequently influence the activity of the calmodulin-

regulated PMCA4. First, we evidenced strong co-localization of calmodulin with CFTR and PMCA4 at the apical membrane of ductal epithelial cells with dSTORM on cross-sections of MPOs **(Figure 13.A.)**. Next, whereas calmodulin strongly associated with the apical membrane in WT MPOs and MLOs, it dissociated from the apical membrane and diffused throughout the cytosol –as suggested by the line intensity profiles– in EtOH-treated or *Cftr* KO MPOs and MLOs **(Figure 13.B, Figure 14. A.)**. Also, similar localisation pattern was observed C*ftr* KO ductal fragments **(Figure 14.B.)**.

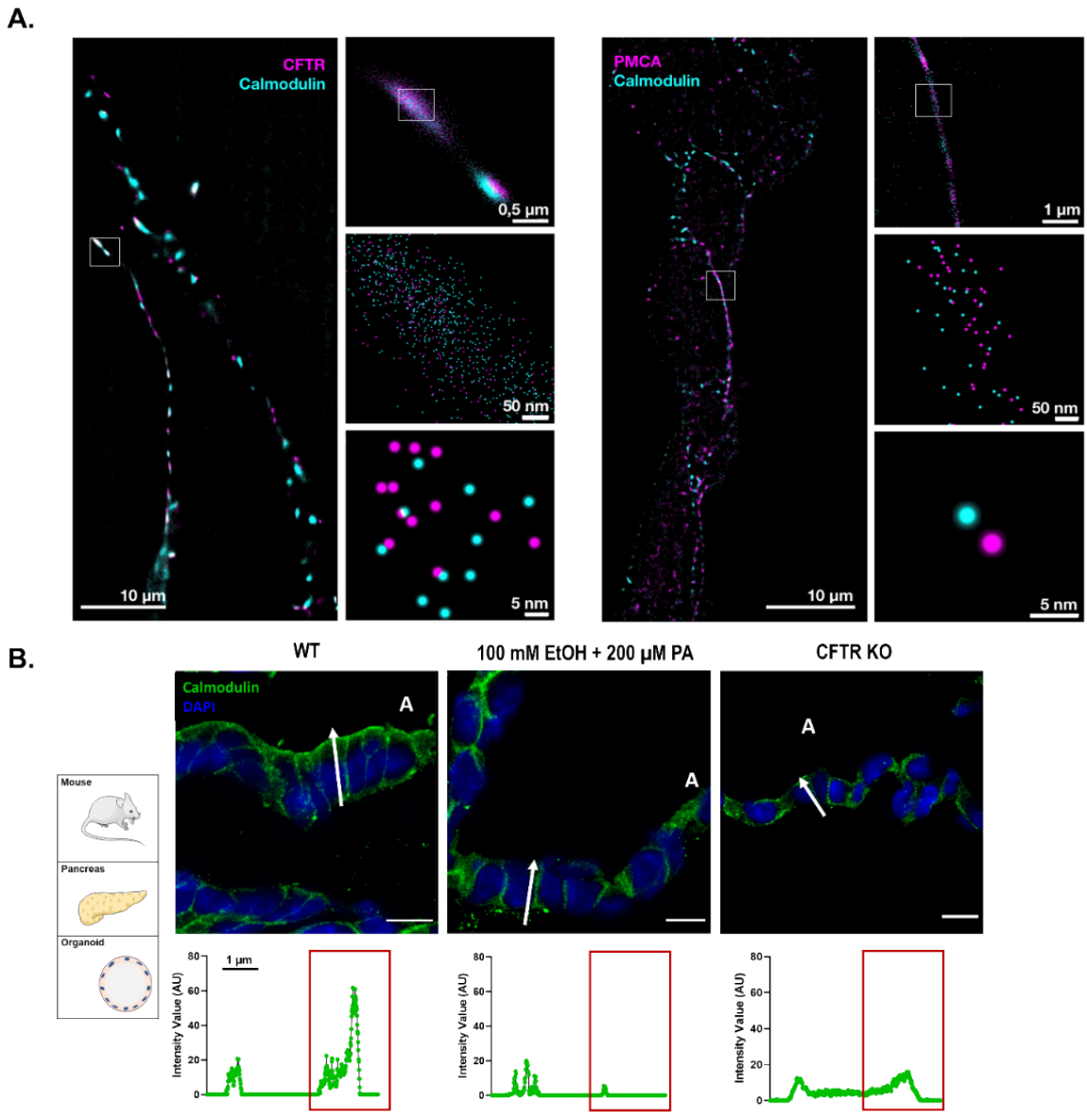

Figure 13. Apical calmodulin recruitment by CFTR regulates PMCA4 activity. A. dSTORM images revealed a strong co-localization of calmodulin with CFTR (left panel) and PMCA4 (right panel) at the apical membrane of ductal epithelial cells on cross-sections of mouse pancreatic ductal organoids **B.** Confocal images and line intensity profiles demonstrate the apical membrane association of calmodulin in WT pancreatic organoids. In EtOH/PA-treated WT and *Cftr* KO cells, this association was lost. Scale bar=10 µm.

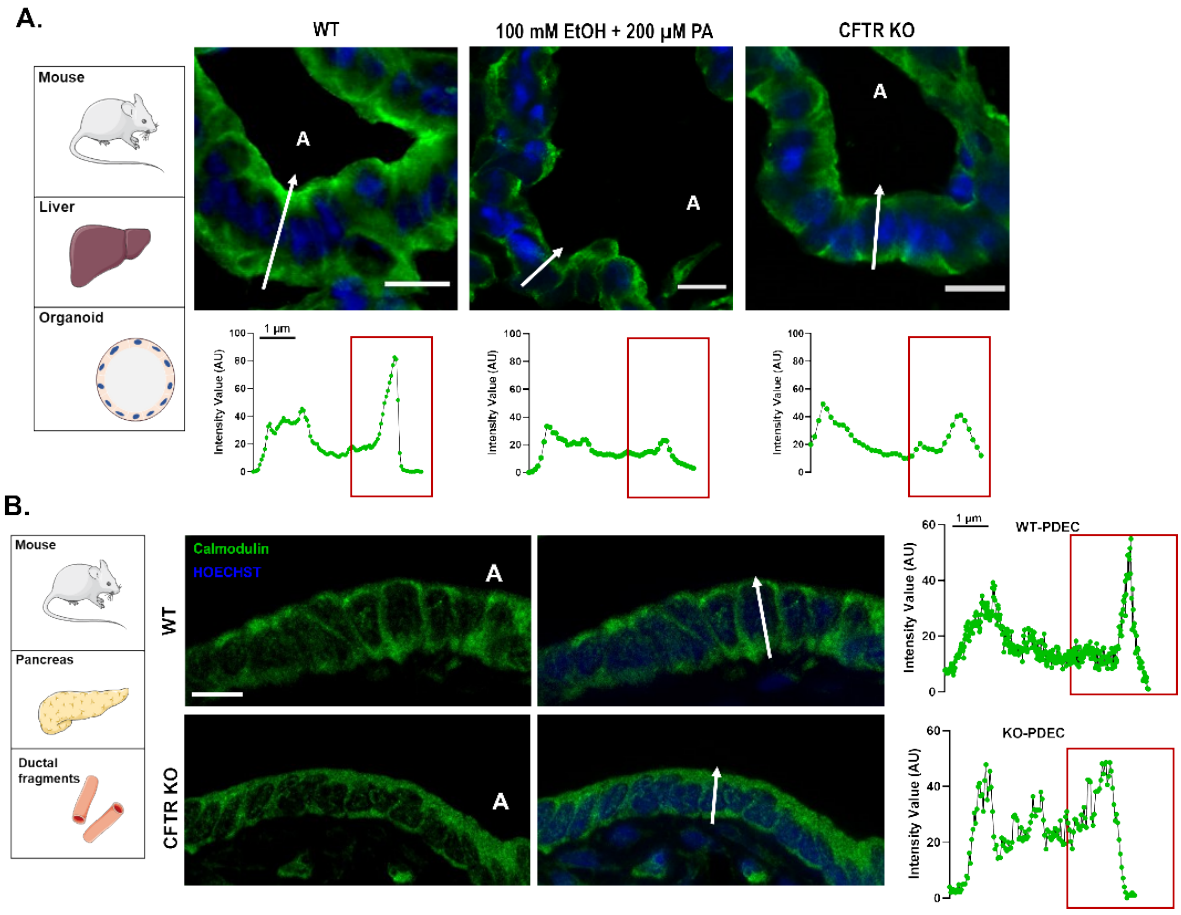

Figure 14. Apical calmodulin recruitment by CFTR regulates PMCA4 activity A. Confocal images and line intensity profiles demonstrate the apical membrane association of calmodulin in WT liver organoids. In EtOH/PA-treated WT and *Cftr* KO cells, this association was lost. Scale bar=10 µm. **B.** Confocal images and line profile analysis of the intracellular distribution of calmodulin in WT and *Cftr* KO pancreatic ductal cells. Calmodulin was strongly associated with the apical membrane in WT ductal epithelial cells, in *Cftr* KO cells this association was lost. A: apical side. Scale bar: 10 µm. n: 3 individual experiments.

Then, we wanted to analyze the effect of impaired calmodulin-CFTR interaction on PMCA4 activity in epithelial cells. As general knockdown or inhibition of calmodulin can have multiple downstream effects, we co-transfected HEK-293 cells with PMCA4 and CFTR or CFTR harboring a mutation in the calmodulin binding site (CFTR(S768A)). Of note, both CFTR and CFTR(S768A) localized to the plasma membrane and co-localized with PMCA4 **(Figure 15.A.)**. While co-transfection of PMCA4 and CFTR markedly increased the slope of Ca^{2+} extrusion, PMCA4 alone showed moderate activity **(Figure 15.B.)**. However, more importantly, cells transfected with CFTR(S768A) showed a significantly impaired PMCA4 activity compared to cells transfected with CFTR. Moreover, dSTORM cluster analysis revealed a 34% reduction of the co-localization ratio between PMCA4-CFTR(S768A)

compared to PMCA4-CFTR **(Figure 15.C-D.)** suggesting that the lack of calmodulin/CFTR interaction is sufficient to decrease PMCA4 activity as well as the stability of the protein nanodomain on the apical plasma membrane.

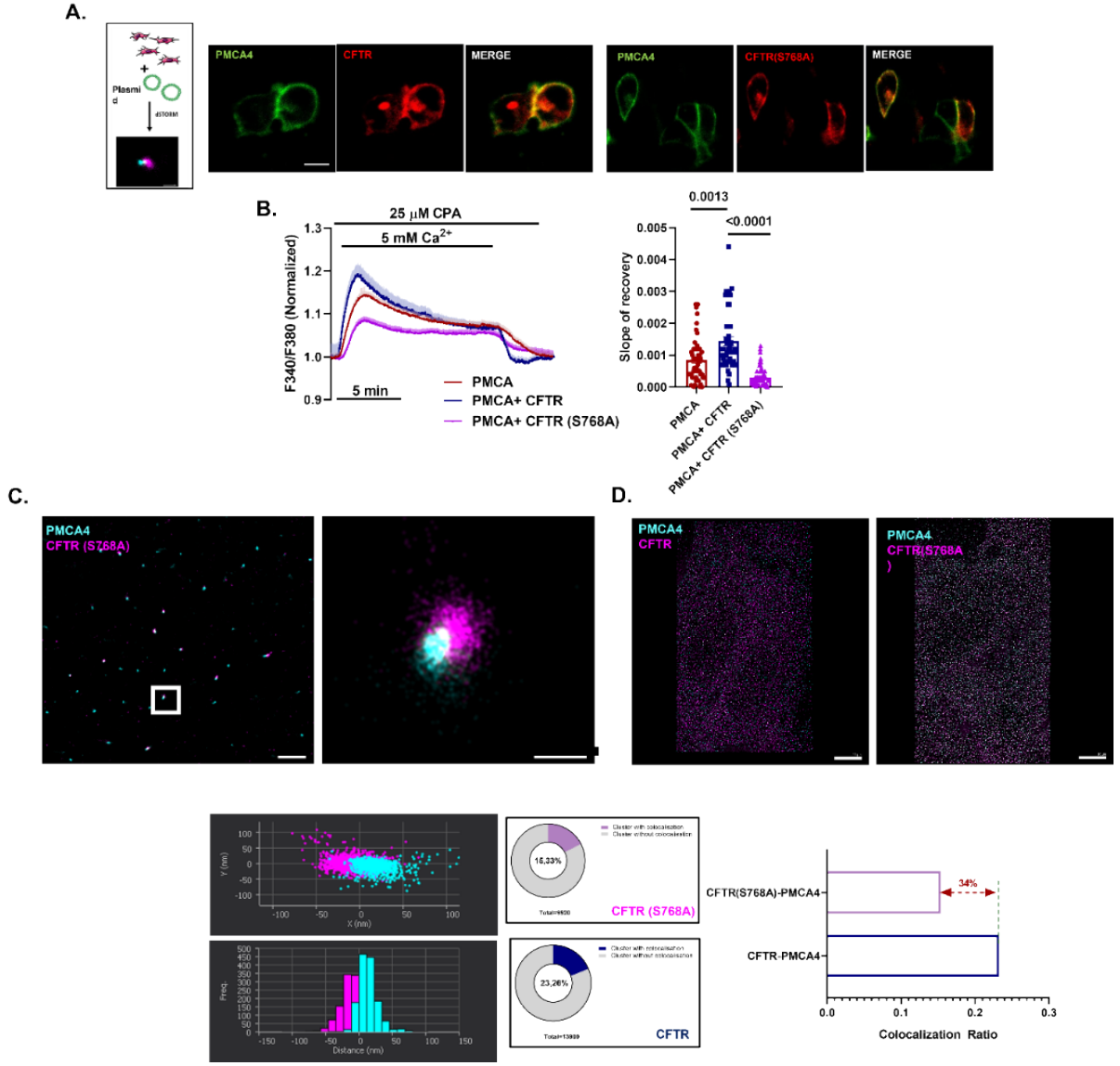

Figure 15. Apical calmodulin recruitment by CFTR regulates PMCA4 activity. A. Confocal images of WT and calmodulin binding site mutant CFTR(S768A) and PMCA4 in transfected HEK-293 cells. **B.** Co-transfection of PMCA4 and CFTR markedly increased the slope of Ca^{2+} extrusion, whereas the calmodulin binding-site mutant CFTR(S768A) significantly impaired the activity of PMCA4. n=4-6 individual experiments. **C.** dSTORM images of HeLa cells transfected with CFTR and PMCA4 revealed a perfect overlap (<20 nm) between the two proteins in the plasma membrane. Scale bars=1μm and 50nm, respectively.**D.** dSTORM images demonstrate the colocalization of calmodulin binding site mutant CFTR and PMCA4 on transfected Hela cells. Scale bars: 10 μm. Cluster analysis of dSTORM images revealed 34% reduction of the co-localization ratio in CFTR(S768A)-PMCA4 compared to CFTR-PMCA4. Scale bars=1μm and 50nm respectively. 5-7 cells were analysed for each condition.

Inhibition of PMCA4 impairs mitochondrial function, increases apoptosis, and results in more severe ethanol-induced acute pancreatitis

Sustained intracellular Ca^{2+} elevation is known to impair mitochondrial function and trigger apoptosis [82]. In the next step we wanted to assess the role of impaired CFTR expression in this phenomenon. Transmission electron microscopy showed no difference in the mitochondrial volume/cell ratio between *Cftr* KO and WT pancreatic ductal cells **(Figure 16.A.)**. Next, administration of 100 µM carbachol resulted in a significant decrease in mitochondrial membrane potential ($\Delta\psi_m$) in EtOH/PA pre-treated and *Cftr* KO–but not in WT– MPOs and MLOs, suggesting that a sustained intracellular Ca^{2+} elevation impairs mitochondrial function in pancreatic ductal cells and cholangiocytes **(Figure 16.B, C, D.)**. This was further tested by comparing the total ketone body concentration in WT and CFTR KO mice **(Figure 16.E.)**. According to our results the total ketone body concentration was increased in the CFTR KO mice, however this difference was not significant. To function properly, the ATPase PMCA4 relies on ATP generated by oxidative phosphorylation and glycolysis. As EtOH decreases the mitochondrial ATP production [35], we inhibited the F1F0-ATPase by oligomycin, which had no effects on the PMCA function in ductal cells **(Figure 16.F.)**.

However, the intracellular distribution of cytochrome c released from the mitochondria –a hallmark of apoptosis– significantly increased in *Cftr* KO compared to WT pancreatic ductal cells, suggesting that sustained Ca^{2+} elevation and disturbed mitochondrial function leads to apoptosis **(Figure 17.A.)**. Additionally, *Cftr* KO pancreatic ductal cells had higher cytoplasmic levels of the initiator caspase 9 compared to WT pancreatic ductal cells, further confirming the increased rate of apoptosis **(Figure 17.B.)**. To further establish the connection between the impaired CFTR expression and mitochondrial function, we measured the intracellular ATP levels in WT control, EtOH/PA-treated and CFTR KO MPOs **(Figure 17.C.)**. This test also confirmed that both EtOH/PA treatment and the lack of CFTR expression impaired the mitochondrial ATP production and thus the cell viability. Finally, by using the PMCA4 inhibitor aurintricarboxylic acid (ATA) in an alcohol-induced pancreatitis mouse model, we aimed to analyse if impaired PMCA4 function could independently enhance the severity of pancreatic and liver diseases. Incubation of pancreatic ductal organoids with 10 µM ATA for 30 min before *in vitro* Ca^{2+} measurements resulted in significantly decreased PMCA4 activity compared to controls, confirming the inhibitory effect of ATA on PMCA4 function **(Figure 17.D.)**.

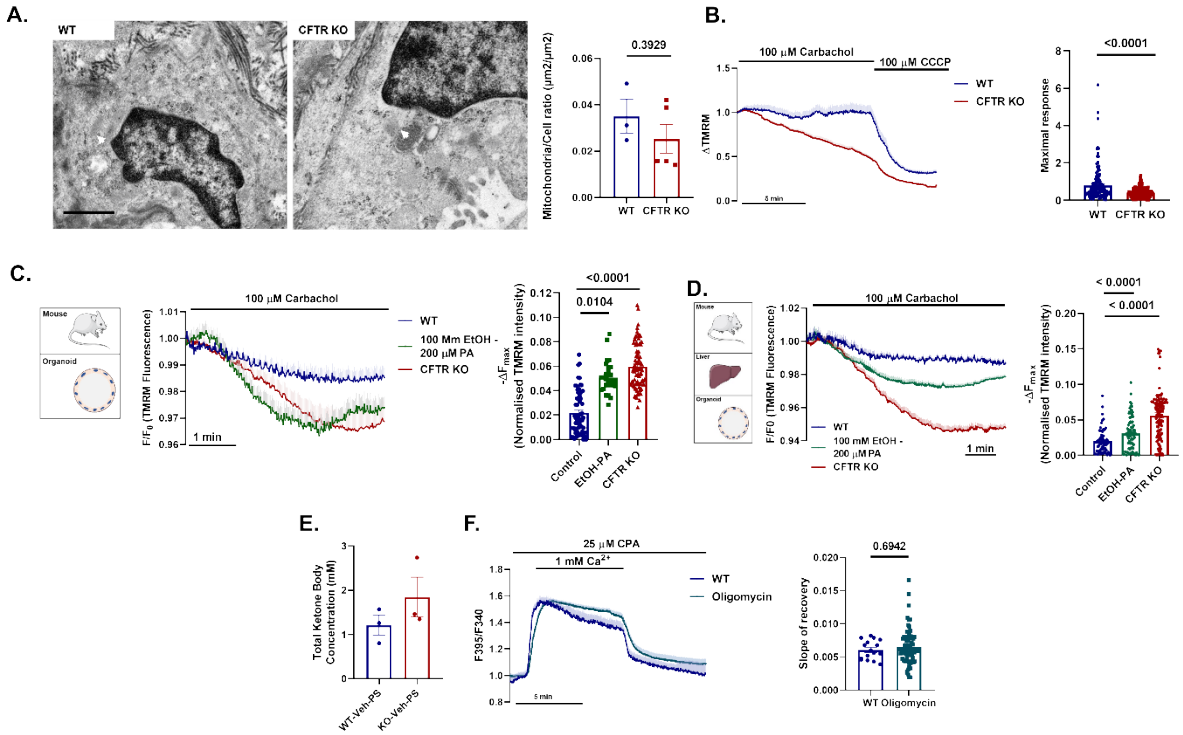

Figure 16. Decreased PMCA4 activity impairs mitochondrial function in mice. A. Representative transmission electron microscopy images of WT and *Cftr* KO mouse pancreatic ductal cells (arrowheads highlight the mitochondria). The mitochondrial volume/cell volume was not changed in *Cftr* KO ductal cell compared to WT. Scale bar: 1 µm. **B-C-D.** Average traces of mitochondrial membrane potential ($\Delta\psi_m$) and maximal fluorescent intensity changes in response to 100 µM carbachol show a significant decrease in the $\Delta\psi_m$ in EtOH/PA pre-treated WT and *Cftr* KO in isolated mouse PDEC, and both mouse pancreatic and liver organoids compared to WT. n=6-10 individual experiments. **E.** Total ketone body concentration was moderately increased in CFTR KO mice; however, the difference was not significant. **F.** Average traces and bar charts demonstrating the effect of the inhibition of mitochondrial ATP production on the Ca^{2+} extrusion in isolated pancreatic ducts. Oligomycin had no effect on the PMCA activity

Finally, by using the PMCA4 inhibitor aurintricarboxylic acid (ATA) in an alcohol-induced pancreatitis mouse model, we aimed to analyse if impaired PMCA4 function could independently enhance the severity of pancreatic and liver diseases. Incubation of pancreatic ductal organoids with 10 µM ATA for 30 min before *in vitro* Ca^{2+} measurements resulted in significantly decreased PMCA4 activity compared to controls, confirming the inhibitory effect of ATA on PMCA4 function **(Figure 18.D.)**. Interestingly, ATA treatment significantly impaired *Pmca4* expression as well, whereas *Pmca1* expression was not changed **(Figure 18.B.)**. Next, a single injection of ATA (intraperitoneally, 5 mg/kg) was administered to WT FVB/N mice 90 min before the first EtOH/POA injection [76]. Compared to vehicle control, ATA pre-treated animals had significantly elevated pancreatic oedema and necrosis scores paralleled with significantly elevated serum amylase activities **(Figure 18.C.)**. Importantly,

CFTR KO mice displayed more severe experimental AP in response to EtOH/PA injection compared to the WT animals, which was not increased further by the ATA treatment **(Supplementary Figure 18.D.)**. Taken together, these results indicate that impaired PMCA4 activity diminish mitochondrial function, augments apoptosis, and potentially increases the severity of CFTR-related pancreatic- and presumably liver diseases.

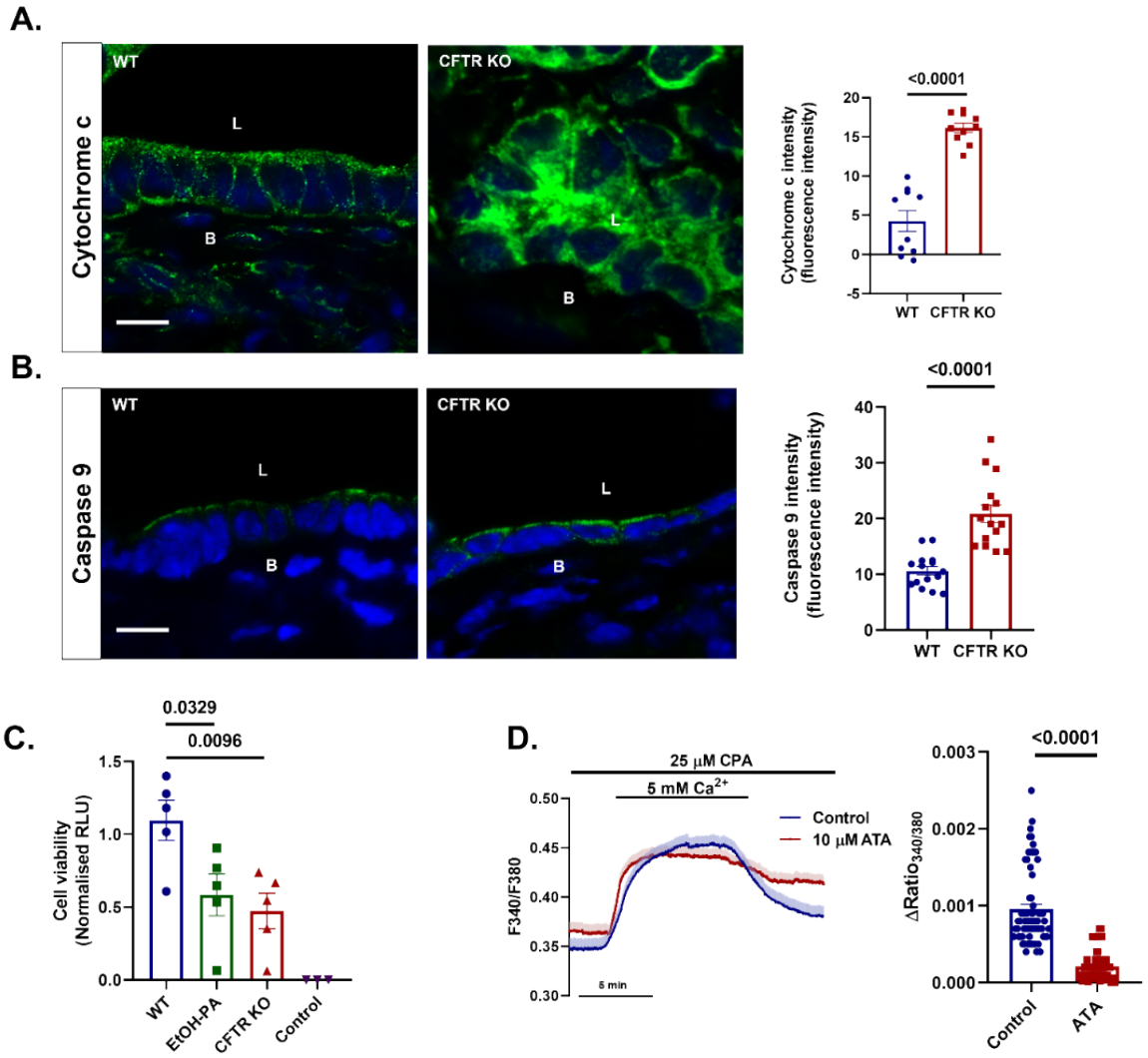

Figure 17. Decreased PMCA function increases apoptosis in mice A. Intracellular distribution of cytochrome c and caspase 9 staining in WT and *Cftr* KO ductal cells. In WT ductal cells cytochrome c showed a granular pattern, whereas in *Cftr* KO cells this was changed to a cytosolic staining. The intensity of caspase 9 staining was increased in *Cftr* KO cells. All averages were calculated from 4-10 individual experiments. Scale bars: 10 µm. **B**: basolateral side; L: lumen. n: 4-10 individual experiments. C. CellTiter-Glo 3D cell viability assay revealed significant decrease of ATP production in EtOH/PA pre-treated WT and CFTR KO MPOs compared to WT. **D.** PMCA4 function of mouse pancreatic organoids was significantly reduced by 30 min pre-incubation with 10 µM ATA *in vitro*.

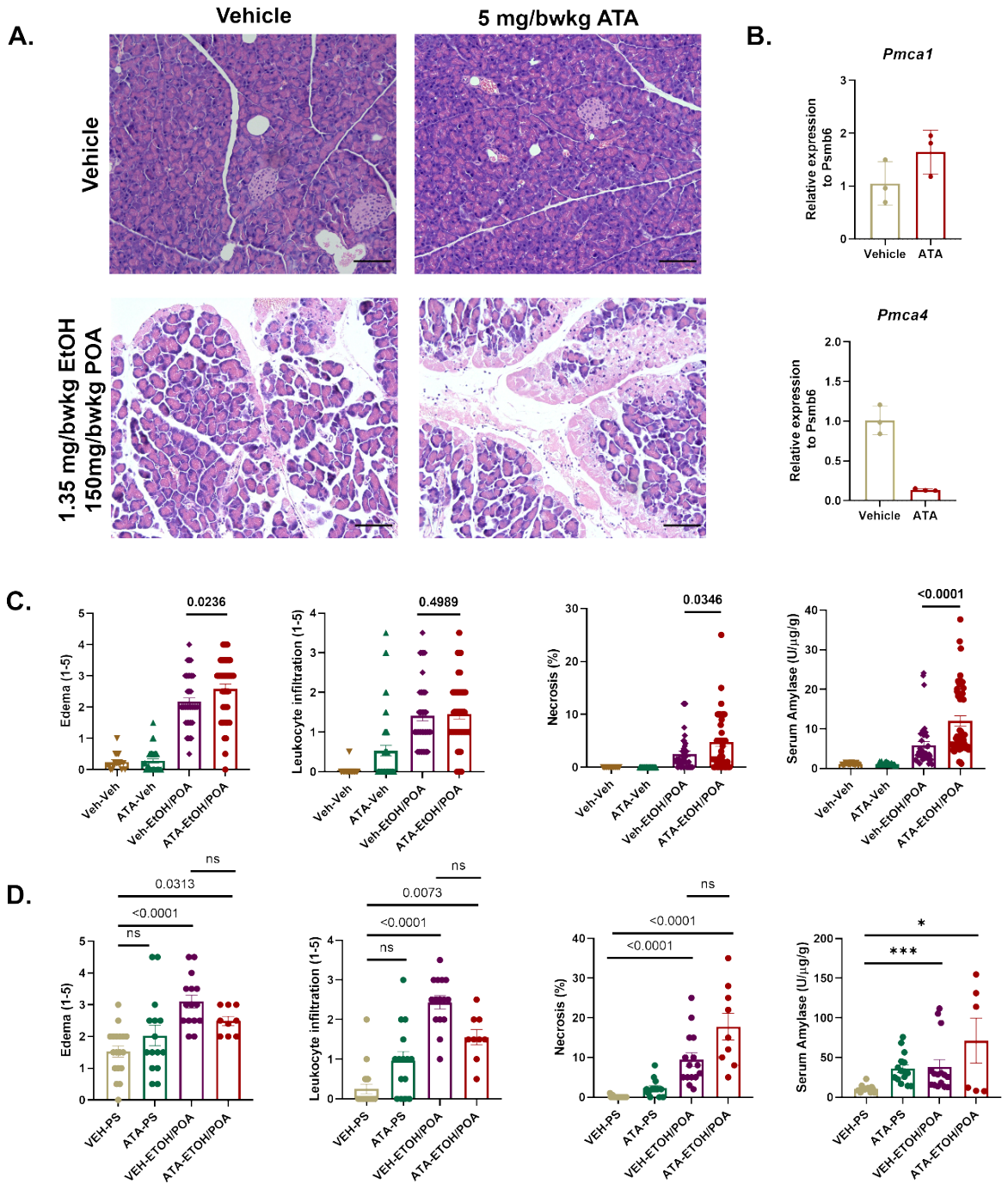

Figure 18. Inhibition of PMCA4 increases the severity of alcohol-induced acute pancreatitis in mice A. Representative H&E images demonstrate the severity of alcohol-induced AP in mice **B.** Gene expression analysis of *Pmca1 and Pmca4* relative to *Psmb6* showed no change of *Pmca1* expression in aurintricarboxylic acid (ATA) treated mice. Interestingly, the expression of *Pmca4* was significantly impaired by ATA treatment. **C.** Histology scores, and serum amylase activities demonstrate the severity of alcohol-induced AP in WT mice. *In vivo* treatment with 5 mg/bwkg ATA significantly elevated the serum amylase activities, oedema, and necrosis scores. n=6-18 animals/group. **D.** Histology scores and serum amylase activities demonstrate the severity of alcohol-induced AP in CFTR KO mice. *In vivo* treatment with 5 mg/bwkg ATA significantly elevated the serum amylase activities, whereas the oedema, leukocyte infiltration and necrosis scores were not elevated further. n=6-18 animals/group.

Discussion

In this study, we provide evidence that impaired CFTR expression –induced by ethanol exposure or genetic mutations and subsequently decreased CFTR-mediated recruitment of calmodulin to the apical membrane attenuates PMCA4 activity and Ca^{2+} extrusion in pancreatic ductal cells and cholangiocytes. The consequent disturbed Ca^{2+} homeostasis leads to damaged mitochondrial function and enhanced apoptosis and ultimately results in increased disease severity. Thus, our results shed light on a novel regulatory mechanism of intracellular Ca^{2+} signaling that might contribute to severity of alcoholic pancreatitis- and hepatitis and potentially to the development of CF-related liver and pancreatic damage.

CFTR is generally considered as a cAMP-activated Cl^- channel, although it may be regulated by $[Ca^{2+}]_i$, or by possible interactions with other components involved in Ca^{2+} homeostasis. However the downstream effects of these interactions on the subcellular signaling events or on the activity of CFTR is not well understood [83,84]. In our study, we first demonstrated that Ca^{2+} extrusion is significantly impaired in ethanol treated and *Cftr* KO pancreatic ductal cells due to diminished PMCA activity. Using several independent *in vitro* model systems, including HPOs and iPSC-derived organoids generated from CF patients, we revealed that the lack of apical CFTR –rather than its function– affects PMCA activity. The fact that diminished CFTR expression did not influence PMCA4 expression or cellular distribution implied a functional interaction between the two proteins. Previously, altered intracellular Ca^{2+} signaling due to elevated IP_3R-dependent Ca^{2+} release and SERCA activity as well as decreased PMCA function was described in cultured bronchial epithelial cells that express F508del CFTR [41,40]. In addition, CF cells display enhanced mitochondrial Ca^{2+} uptake compared to controls [85]. Importantly, correction of CFTR expression with VX-809 in this model seemed to restore the intracellular Ca^{2+} signaling alterations [86]. Besides increased intracellular Ca^{2+} release and impaired Ca^{2+} clearance, increased activity of extracellular Ca^{2+} influx is described in CF. Antigny *et al.* demonstrated that transient receptor potential canonical 6 (TRPC6) channel-dependent extracellular Ca^{2+} influx is increased in CF airway cells [87]. Moreover, Balghi *et al.* indicated that Orai1-mediated extracellular Ca^{2+} influx is equally increased in CF airway cells leading to increased secretion of the proinflammatory cytokine IL-8 [88]. On the other hand, sustained intracellular Ca^{2+} overload is a hallmark of AP. The most frequent pathogenic factors –including bile acids or non-oxidative EtOH metabolites– trigger the release of ER Ca^{2+} stores and activate extracellular Ca^{2+} influx

leading to impaired fluid and HCO_3^- secretion [89,90]. The subsequent sustained intracellular Ca^{2+} overload triggers mitochondrial damage with consequent ATP depletion and cell damage [91], further impairing ATP-dependent Ca^{2+} extrusion.

AH is a potentially lethal complication of alcoholic liver disease, which has been attributed to hepatocellular damage in the past [36]. Recently, binding of neutrophils to ITGB1 expressed on the cell surface of cholangiocytes was shown to contribute to epithelial cell damage and the development of cholestasis in AH [38]. Other studies showed that cholestatic liver injury can be involved in the pathogenesis of AH, moreover, impaired secretion by cholangiocytes, or cholestasis, results in a worse outcome [37]. In addition, other liver diseases – such as primary biliary cholangitis, primary sclerosing cholangitis, or cystic fibrosis-related liver disease (CFRD)– are associated with dysfunctional cholangiocyte secretion [92]. This previously unrecognised contribution of cholangiocyte damage in AH altered our understanding of the disease pathogenesis and offers novel therapeutic strategies. A previous study described that stimulation of Toll-like receptor 4 by lipopolysaccharides activates NF-κB to down-regulate type 3 inositol trisphosphate receptor expression in human cholangiocytes, which may contribute to the cholestasis observed in AH [92]. However, this was not directly caused by ethanol exposure. Proper cholangiocyte secretion largely depends on efficient functioning of CFTR located at the apical membrane of these cells [39,93]. As EtOH and its metabolites damage the expression and function of CFTR in pancreatic ductal epithelial cells [35], it seems plausible that alcohol-induced CFTR damage may contribute to the development of cholangiocyte dysfunction and cholestasis in AH. In this study, we demonstrated significantly decreased apical plasma membrane CFTR expression accompanied with a significantly impaired CFTR activity in post-mortem AH patient liver samples and apical diminished Cl^-/HCO_3^- exchange upon alcohol exposure in mouse liver organoids. In addition, both EtOH pre-incubated WT and *Cftr* KO liver organoids displayed impaired Ca^{2+} extrusion due to decreased PMCA activity. The lack of CFTR-mediated secretion as well as altered intracellular Ca^{2+} homeostasis can damage the cholangiocyte secretion contributing to the development of AH-related cholestasis and potentially CF-related liver disease (CFLD) and severely worsen the clinical outcome.

In our experiments, we demonstrated that PMCA4 co-localizes with CFTR at the apical membrane of ductal cells in multiple models. Moreover, using super-resolution dSTORM, we highlighted that CFTR and PMCA4 are within 20 nm distance suggesting a physical interaction of the two proteins. Previously, the co-immunoprecipitation experiments of Philippe *et al.* suggested that CFTR interacts with SERCA and PMCA in airway epithelial

cells, although the nature of this interaction was not revealed [41]. Recently, Bozoky *et al.* demonstrated increased open probability of CFTR due to direct binding of calmodulin to its R domain [43], which provided a novel mechanism for the regulation of intracellular Ca^{2+}-mediated CFTR activity. Interestingly, the authors proved that calmodulin binds to CFTR in an alternative binding conformation allowing the two lobes of calmodulin to independently bind two separate sequences. This binding conformation may allow CFTR to recruit calmodulin and subsequently determine the activity of other calmodulin-regulated proteins such as PMCA isoforms in a macromolecular complex at the apical plasma membrane. Binding of Ca^{2+}-calmodulin with the calmodulin binding domain of PMCA competitively antagonizes the autoinhibitory domain leading to PMCA activation [94]. In untreated WT pancreatic- and liver organoids, calmodulin was associated with the apical membrane and strongly co-localized with CFTR and PMCA4. In *Cftr* KO- and ethanol-treated organoids, this apical localization was lost suggesting that the presence of CFTR at the apical membrane is necessary to recruit calmodulin. To verify that interaction of calmodulin with CFTR is required for PMCA activation, we overexpressed a calmodulin-binding site mutant of CFTR (CFTR(S768A)) and PMCA4 in HEK-293 cells and showed significantly impaired Ca^{2+} extrusion, whereas the interaction between CFTR and PMCA4 also remarkably decreased.

During the pathogenesis of alcohol-induced AP, it is well-established that acute exposure of acinar [95] and ductal cells [35] to ethanol or ethanol metabolites induce sustained elevation of $[Ca^{2+}]_i$ leading to the opening of the mitochondrial permeability transition pore dissipating $\Delta\Psi_m$ with a consequent drop of ATP synthesis [96,97]. In our experiments, instead of acute administration, we incubated the ductal cells overnight, which may model the effects ethanol consumption better. Although we found no evidence for mitochondrial morphological damage but detected a remarkable drop of $\Delta\Psi_m$ when challenging the ethanol treated and *Cftr* KO MPOs with carbachol. In addition, increased cytosolic staining for cytochrome c and caspase 9 in *Cftr* KO ductal cells suggested increased apoptosis. Finally, PMCA4 inhibition in an *in vivo* model of alcoholic AP significantly increased disease severity suggesting that impaired PMCA4 function due to impaired CFTR expression by itself can contribute to cell damage in alcoholic pancreatitis and hepatitis. Importantly, our results highlight that restoration of PMCA activity or enhancement of the Ca^{2+} extrusion can have potential therapeutic benefit not only in alcoholic pancreatitis and hepatitis, but also in cystic fibrosis related liver disease and pancreatitis. We demonstrated that restoration of CFTR expression with correctors can also improve the function of PMCA. Effectivity of triple combination therapy for CF patients was shown recently [98] and persistent improvement of pancreatic

function was reported in CF patients receiving ivacaftor [99]. Moreover, prevention of intracellular Ca^{2+} overload with pharmacologic inhibition of Orai1 resulted in favorable clinical outcomes among patients with severe AP [100]. As an example, in a recent study the phenothiazine methylene blue (MB) was shown to stimulate PMCA activity in neural cultures and in human tissues from Alzheimer's disease-affected brain [101]. As MB is used to treat methemoglobinemia and other diseases [102], it could be utilized in alcohol-induced hepatitis and pancreatitis and in CFLD and pancreatic diseases as well.

Taken together, in this study we identified a novel regulatory interaction based on the apical recruitment of calmodulin by CFTR determining the activity of PMCA4 and intracellular Ca^{2+} extrusion in polarized epithelial cells. Thus, prevention of the intracellular Ca^{2+} overload with improving PMCA activity might represent a novel potential drug target in alcoholic pancreatitis and -hepatitis and in CFTR-related diseases, such as CFLD, CF-related pancreatic disease.

Summary

Alcoholic pancreatitis and hepatitis are frequent, potentially lethal diseases with limited treatment options. Our previous study reported that the expression of CFTR Cl^- channel is impaired by ethanol in pancreatic ductal cells leading to more severe alcohol-induced pancreatitis. In addition to determining epithelial ion secretion, CFTR has multiple interactions with other proteins, which may influence intracellular Ca^{2+} signaling. Thus, we aimed to investigate the impact of ethanol mediated CFTR damage on intracellular Ca^{2+} homeostasis in pancreatic ductal epithelial cells and cholangiocytes. Human and mouse pancreas and liver samples and *ex vivo* organoids were used to study ion secretion, intracellular signaling and protein expression and interaction. The effect of PMCA4 inhibition was analysed in a mouse model of alcohol-induced pancreatitis. Our findings show the decreased CFTR expression impaired PMCA function and resulted in sustained intracellular Ca^{2+} elevation in ethanol-treated and mouse and human pancreatic organoids. Liver samples from alcoholic hepatitis patients and ethanol-treated mouse liver organoids showed decreased CFTR expression and function, and impaired PMCA4 activity. PMCA4 co-localizes and physically interacts with CFTR on the apical membrane of polarized epithelial cells, where CFTR-dependent calmodulin recruitment determines PMCA4 activity. The sustained intracellular Ca^{2+} elevation in the absence of CFTR inhibited mitochondrial function and was accompanied with increased apoptosis in pancreatic epithelial cells and PMCA4 inhibition increased the severity of alcohol-induced AP in mice. In conclusion our results suggest that improving Ca^{2+} extrusion in epithelial cells may be a potential novel therapeutic approach to protect the exocrine pancreatic function in alcoholic pancreatitis and prevent the development of cholestasis in alcoholic hepatitis

Novel observations:

- We have provided evidence that impaired CFTR expression –induced by ethanol exposure or genetic mutations and subsequently decreased CFTR-mediated recruitment of calmodulin to the apical membrane attenuates PMCA4 activity and Ca^{2+} extrusion in pancreatic ductal cells and cholangiocytes.
- The consequent disturbed Ca^{2+} homeostasis leads to damaged mitochondrial function and enhanced apoptosis and ultimately results in increased disease severity. Thus, our results shed light on a novel regulatory mechanism of intracellular Ca^{2+} signaling that might contribute to severity of alcoholic pancreatitis- and hepatitis and potentially to the development of CF-related liver and pancreatic damage.

Acknowledgements

I would like to express my most sincere gratitude to my mentor József Maléth at the First Department of Medicine, University of Szeged for his guidance and support. Without his outstanding supervision, this Ph.D. thesis would not have been possible. I owe a special thanks to Dr. Pallagi Petra for her collaboration, help and valuable insight through all these years. I also would like to thank Prof. Dr. Peter Hegyi, Prof. Dr. Zoltán Rakonczay Jr. and Dr. Viktória Venglovecz for their scientific advice. I am grateful to Prof. Dr. Csaba Lengyel and Prof. Dr. György Ábrahám, the current and former head of First Department of Medicine, University of Szeged and Prof. Dr. Varró András (former head of Department of Pharmacology and Pharmacotherapy University of Szeged) who gave me the opportunity to work at their departments. I would also like to thank my colleagues and friends, Árpád Varga, Viktoria Szabó, Boldizsár Jójárt, Noémi Papp, Aletta Kiss, Tünde Molnár, Petra Susánszky, Tim Crul, Bálint Tél Ingrid Sendstad, Emese Réka Bálint, Dr. Zsolt Balla, Marietta Görög, Xénia Katona, Margit Németh, Réka Molnár, Emese Tóth, Júlia Fanczal, Dr. Balázs Kui, Dr Balázs Németh, Máté Katona for all the help, encouragement, and the great times we had.This work would not have been possible to accomplish without the assistance and work of Krisztina Dudás, Melinda Molnár, Zsuzsanna Konczos, Edit Magyarné Pálfi, Tünde Pritz, Rea Fritz, Miklósné Árva. I am deeply grateful to Professor Alexander Kleger, Ulm, Germany, and his research team for the fruitful collaboration and to Professor Ursula Seidler (Department of Gastroenterology, Hannover Medical School, Hanover, Germany) for providing us the *Cftr* KO mice. I also would like to thank Professor Gergely Lukács (Department of Physiology, McGill University, Montréal, Canada) for providing us the CFTR-3xHA plasmid and Mike Gray (University of Newcastle, Newcastle, UK) for his kind gift of CFPAC-1 cells. I owe warm thanks to my beloved family for the unconditional love, support, and patience throughout my doctorate; my husband Gábor Szabó, my dad Prof. Dr. László Madácsy, my mom Terézia Siskó, my grandparents id. Prof. Dr. László Madácsy, Dr. Attila Kiss and Dr. Adrienne Polgár who taught me of the world and encouraged me to devote myself science.

References

1. Hong, J. H., Park, S., Shcheynikov, N. & Muallem, S. Mechanism and synergism in epithelial fluid and electrolyte secretion. *Pflugers Arch.* **466**, 1487–1499 (2014).
2. Hegyi, P. & Petersen, O. H. The exocrine pancreas: the acinar-ductal tango in physiology and pathophysiology. Rev. Physiol. Biochem. Pharmacol. 165, 1–30 (2013).
3. LAM (Lege Artis Medicinæ)- A pancreas-vezetéksejtek bikarbonátszekréciójának szerepe akut pancreatitisben. http://www.elitmed.hu/kiadvanyaink/lam_lege_artis_medicin/a_pancreas_vezeteksejtek_bikarbonatszekreciojanak_szerepe_akut_pancreatitisben_5819/.
4. ISHIGURO, H. *et al.* PHYSIOLOGY AND PATHOPHYSIOLOGY OF BICARBONATE SECRETION BY PANCREATIC DUCT EPITHELIUM. *Nagoya J. Med. Sci.* **74**, 1–18 (2012).
5. Voronina, S., Longbottom, R., Sutton, R., Petersen, O. H. & Tepikin, A. Bile acids induce calcium signals in mouse pancreatic acinar cells: implications for bile-induced pancreatic pathology. *J. Physiol.* **540**, 49–55 (2002).
6. Shcheynikov, N. *et al.* The Slc26a4 transporter functions as an electroneutral Cl-/I-/HCO3- exchanger: role of Slc26a4 and Slc26a6 in I- and HCO3- secretion and in regulation of CFTR in the parotid duct. *J. Physiol.* **586**, 3813–3824 (2008).
7. Pallagi, P. *et al.* Trypsin reduces pancreatic ductal bicarbonate secretion by inhibiting CFTR Cl^- channels and luminal anion exchangers. *Gastroenterology* **141**, 2228-2239.e6 (2011).
8. Pallagi, P. *et al.* The role of pancreatic ductal secretion in protection against acute pancreatitis in mice*. *Crit. Care Med.* **42**, e177-188 (2014).
9. Hegyi, P., Maléth, J., Venglovecz, V. & Rakonczay, Z. Pancreatic ductal bicarbonate secretion: challenge of the acinar Acid load. *Front. Physiol.* **2**, 36 (2011).
10. Kerem, B. *et al.* Identification of the cystic fibrosis gene: genetic analysis. *Science* **245**, 1073–1080 (1989).
11. Riordan, J. R. *et al.* Identification of the cystic fibrosis gene: cloning and characterization of complementary DNA. *Science* **245**, 1066–1073 (1989).
12. Madácsy, T., Pallagi, P. & Maleth, J. Cystic Fibrosis of the Pancreas: The Role of CFTR Channel in the Regulation of Intracellular Ca2+ Signaling and Mitochondrial Function in the Exocrine Pancreas. *Front. Physiol.* **9**, 1585 (2018).
13. Vankeerberghen, A., Cuppens, H. & Cassiman, J.-J. The cystic fibrosis transmembrane conductance regulator: an intriguing protein with pleiotropic functions. *J. Cyst. Fibros. Off. J. Eur. Cyst. Fibros. Soc.* **1**, 13–29 (2002).
14. Callebaut, I., Chong, P. A. & Forman-Kay, J. D. CFTR structure. *J. Cyst. Fibros. Off. J. Eur. Cyst. Fibros. Soc.* **17**, S5–S8 (2018).
15. Liu, F., Zhang, Z., Csanády, L., Gadsby, D. C. & Chen, J. Molecular Structure of the Human CFTR Ion Channel. *Cell* **169**, 85-95.e8 (2017).
16. Guggino, W. B. & Stanton, B. A. New insights into cystic fibrosis: molecular switches that regulate CFTR. *Nat. Rev. Mol. Cell Biol.* **7**, 426–436 (2006).
17. Sheppard, D. N. & Welsh, M. J. Structure and function of the CFTR chloride channel. *Physiol. Rev.* **79**, S23-45 (1999).
18. Bradbury, N. A. Intracellular CFTR: localization and function. *Physiol. Rev.* **79**, S175-191 (1999).
19. Quinton, P. M. Role of epithelial HCO3− transport in mucin secretion: lessons from cystic fibrosis. *Am. J. Physiol. - Cell Physiol.* **299**, C1222–C1233 (2010).

20. Lee, M. G., Ohana, E., Park, H. W., Yang, D. & Muallem, S. Molecular Mechanism of Pancreatic and Salivary Glands Fluid and HCO3− Secretion. *Physiol. Rev.* **92**, 39–74 (2012).
21. Hegyi, P. *et al.* CFTR: A New Horizon in the Pathomechanism and Treatment of Pancreatitis. *Rev. Physiol. Biochem. Pharmacol.* (2016) doi:10.1007/112_2015_5002.
22. Park, H. W. *et al.* Dynamic regulation of CFTR bicarbonate permeability by [Cl-]i and its role in pancreatic bicarbonate secretion. *Gastroenterology* **139**, 620–631 (2010).
23. Ooi, C. Y. & Durie, P. R. Cystic fibrosis transmembrane conductance regulator (CFTR) gene mutations in pancreatitis. *J. Cyst. Fibros. Off. J. Eur. Cyst. Fibros. Soc.* **11**, 355–362 (2012).
24. Ooi, C. Y. *et al.* Type of CFTR mutation determines risk of pancreatitis in patients with cystic fibrosis. *Gastroenterology* **140**, 153–161 (2011).
25. Sharer, N. *et al.* Mutations of the cystic fibrosis gene in patients with chronic pancreatitis. *N. Engl. J. Med.* **339**, 645–652 (1998).
26. Cohn, J. A. *et al.* Relation between mutations of the cystic fibrosis gene and idiopathic pancreatitis. *N. Engl. J. Med.* **339**, 653–658 (1998).
27. Maléth, J. *et al.* Alcohol Disrupts Levels and Function of the Cystic Fibrosis Transmembrane Conductance Regulator to Promote Development of Pancreatitis. *Gastroenterology* **148**, 427-439.e16 (2015).
28. Judák, L. *et al.* Ethanol and its non-oxidative metabolites profoundly inhibit CFTR function in pancreatic epithelial cells which is prevented by ATP supplementation. *Pflüg. Arch. Eur. J. Physiol.* **466**, 549–562 (2014).
29. Dimagno, M. J. *et al.* A proinflammatory, antiapoptotic phenotype underlies the susceptibility to acute pancreatitis in cystic fibrosis transmembrane regulator (-/-) mice. *Gastroenterology* **129**, 665–681 (2005).
30. Ko, S. B. H. *et al.* Corticosteroids correct aberrant CFTR localization in the duct and regenerate acinar cells in autoimmune pancreatitis. *Gastroenterology* **138**, 1988–1996 (2010).
31. Ko, S. B. H. *et al.* Molecular mechanisms of pancreatic stone formation in chronic pancreatitis. *Front. Physiol.* **3**, 415 (2012).
32. World Health Organization. Global status report on alcohol and health 2018. (2018).
33. Yadav, D. & Lowenfels, A. B. The epidemiology of pancreatitis and pancreatic cancer. *Gastroenterology* **144**, 1252–1261 (2013).
34. Párniczky, A. *et al.* Prospective, Multicentre, Nationwide Clinical Data from 600 Cases of Acute Pancreatitis. *PloS One* **11**, e0165309 (2016).
35. Maléth, J. *et al.* Alcohol disrupts levels and function of the cystic fibrosis transmembrane conductance regulator to promote development of pancreatitis. *Gastroenterology* **148**, 427-439.e16 (2015).
36. Lucey, M. R., Mathurin, P. & Morgan, T. R. Alcoholic hepatitis. *N. Engl. J. Med.* **360**, 2758–2769 (2009).
37. Altamirano, J. *et al.* A histologic scoring system for prognosis of patients with alcoholic hepatitis. *Gastroenterology* **146**, 1231-1239.e1–6 (2014).
38. Takeuchi, M. *et al.* Neutrophils interact with cholangiocytes to cause cholestatic changes in alcoholic hepatitis. *Gut* **70**, 342–356 (2021).
39. Trampert, D. C. & Nathanson, M. H. Regulation of bile secretion by calcium signaling in health and disease. *Biochim. Biophys. Acta Mol. Cell Res.* **1865**, 1761–1770 (2018).
40. Antigny, F., Norez, C., Cantereau, A., Becq, F. & Vandebrouck, C. Abnormal spatial diffusion of Ca2+ in F508del-CFTR airway epithelial cells. *Respir. Res.* **9**, 70 (2008).
41. Philippe, R. *et al.* SERCA and PMCA pumps contribute to the deregulation of Ca2+ homeostasis in human CF epithelial cells. *Biochim. Biophys. Acta* **1853**, 892–903 (2015).

42. Maléth, J. & Hegyi, P. Ca2+ toxicity and mitochondrial damage in acute pancreatitis: translational overview. *Philos. Trans. R. Soc. Lond. B. Biol. Sci.* **371**, 20150425 (2016).
43. Bozoky, Z. *et al.* Synergy of cAMP and calcium signaling pathways in CFTR regulation. *Proc. Natl. Acad. Sci. U. S. A.* **114**, E2086–E2095 (2017).
44. Ahuja, M., Jha, A., Maléth, J., Park, S. & Muallem, S. cAMP and Ca2+ signaling in secretory epithelia: Crosstalk and Synergism. *Cell Calcium* **55**, 385–393 (2014).
45. Argent, B. E., Gray, M. A., Steward, M. C. & Case, R. M. *Physiology of the Gastrointestinal Tract.* (Elsevier).
46. Wang, Y. *et al.* Regulation of CFTR channels by HCO3−-sensitive soluble adenylyl cyclase in human airway epithelial cells. *Am. J. Physiol.-Cell Physiol.* **289**, C1145–C1151 (2005).
47. Namkung, W. *et al.* Ca2+ Activates Cystic Fibrosis Transmembrane Conductance Regulator- and Cl−-dependent HCO Transport in Pancreatic Duct Cells. *J. Biol. Chem.* **278**, 200–207 (2003).
48. A functional CFTR protein is required for mouse intestinal cAMP-, cGMP- and Ca(2+)-dependent HCO3- secretion. https://www.ncbi.nlm.nih.gov/pmc/articles/PMC1160074/.
49. Rasmussen, J. E., Sheridan, J. T., Polk, W., Davies, C. M. & Tarran, R. Cigarette Smoke-induced Ca2+ Release Leads to Cystic Fibrosis Transmembrane Conductance Regulator (CFTR) Dysfunction. *J. Biol. Chem.* **289**, 7671–7681 (2014).
50. Park, S. *et al.* Irbit Mediates Synergy Between Ca2+ and cAMP Signaling Pathways During Epithelial Transport in Mice. *Gastroenterology* **145**, 232–241 (2013).
51. Bozoky, Z. *et al.* Synergy of cAMP and calcium signaling pathways in CFTR regulation. *Proc. Natl. Acad. Sci. U. S. A.* **114**, E2086–E2095 (2017).
52. Balghi, H. *et al.* Enhanced Ca2+ entry due to Orai1 plasma membrane insertion increases IL-8 secretion by cystic fibrosis airways. *FASEB J.* **25**, 4274–4291 (2011).
53. Philippe, R. *et al.* SERCA and PMCA pumps contribute to the deregulation of Ca2+ homeostasis in human CF epithelial cells. *Biochim. Biophys. Acta BBA - Mol. Cell Res.* **1853**, 892–903 (2015).
54. Shapiro, B. L. Mitochondrial dysfunction, energy expenditure, and cystic fibrosis. *Lancet Lond. Engl.* **2**, 289 (1988).
55. Valdivieso, A. G. & Santa-Coloma, T. A. CFTR activity and mitochondrial function. *Redox Biol.* **1**, 190–202 (2013).
56. Antigny, F., Norez, C., Becq, F. & Vandebrouck, C. Calcium homeostasis is abnormal in cystic fibrosis airway epithelial cells but is normalized after rescue of F508del-CFTR. *Cell Calcium* **43**, 175–183 (2008).
57. Donnell, G. N. & Cleland, R. S. Intestinal atresia or stenosis in the newborn associated with fibrocystic disease of the pancreas. *California Medicine* 165–170 (1961).
58. Antigny, F. *et al.* Dysfunction of mitochondria Ca2+ uptake in cystic fibrosis airway epithelial cells. *Mitochondrion* **9**, 232–241 (2009).
59. Maléth, J. *et al.* Non-conjugated chenodeoxycholate induces severe mitochondrial damage and inhibits bicarbonate transport in pancreatic duct cells. *Gut* **60**, 136–138 (2011).
60. Central role of mitochondrial injury in the pathogenesis of acute pancreatitis - Maléth - 2013 - Acta Physiologica - Wiley Online Library. https://onlinelibrary.wiley.com/doi/abs/10.1111/apha.12037.
61. (13) Golstein P, Kroemer G.. Cell death by necrosis: towards a molecular definition. Trends Biochem Sci 32: 37-43. *ResearchGate* https://www.researchgate.net/publication/6656505_Golstein_P_Kroemer_G_Cell_death_by_necrosis_towards_a_molecular_definition_Trends_Biochem_Sci_32_37-43.

62. Jendrossek, V. *et al.* Apoptotic response of Chang cells to infection with Pseudomonas aeruginosa strains PAK and PAO-I: molecular ordering of the apoptosis signaling cascade and role of type IV pili. *Infect. Immun.* **71**, 2665–2673 (2003).
63. Phospholipase A2 Functions in Pseudomonas aeruginosa- Induced Apoptosis. http://iai.asm.org/content/74/2/850.abstract.
64. l'Hoste, S. *et al.* CFTR mediates apoptotic volume decrease and cell death by controlling glutathione efflux and ROS production in cultured mice proximal tubules. *Am. J. Physiol. Renal Physiol.* **298**, F435-453 (2010).
65. Rottner, M. *et al.* Increased Oxidative Stress Induces Apoptosis in Human Cystic Fibrosis Cells. *PLOS ONE* **6**, e24880 (2011).
66. Exaggerated apoptosis and NF-κB activation in pancreatic and tracheal cystic fibrosis cells | The FASEB Journal. https://www.fasebj.org/doi/abs/10.1096/fj.06-7614com.
67. Vij, N., Fang, S. & Zeitlin, P. L. Selective Inhibition of Endoplasmic Reticulum-associated Degradation Rescues ΔF508-Cystic Fibrosis Transmembrane Regulator and Suppresses Interleukin-8 Levels THERAPEUTIC IMPLICATIONS. *J. Biol. Chem.* **281**, 17369–17378 (2006).
68. Bozoky, Z. *et al.* Synergy of cAMP and calcium signaling pathways in CFTR regulation. *Proc. Natl. Acad. Sci. U. S. A.* **114**, E2086–E2095 (2017).
69. Maléth, J., Choi, S., Muallem, S. & Ahuja, M. Translocation between PI(4,5)P2-poor and PI(4,5)P2-rich microdomains during store depletion determines STIM1 conformation and Orai1 gating. *Nat. Commun.* **5**, 5843 (2014).
70. Rakonczay, Z. *et al.* CFTR gene transfer to human cystic fibrosis pancreatic duct cells using a Sendai virus vector. *J. Cell. Physiol.* **214**, 442–455 (2008).
71. Ratcliff, R. *et al.* Production of a severe cystic fibrosis mutation in mice by gene targeting. *Nat. Genet.* **4**, 35–41 (1993).
72. Molnár, R. *et al.* Mouse pancreatic ductal organoid culture as a relevant model to study exocrine pancreatic ion secretion. *Lab. Investig. J. Tech. Methods Pathol.* **100**, 84–97 (2020).
73. Hohwieler, M. *et al.* Human pluripotent stem cell-derived acinar/ductal organoids generate human pancreas upon orthotopic transplantation and allow disease modelling. *Gut* **66**, 473–486 (2017).
74. Maléth, J. *et al.* Alcohol disrupts levels and function of the cystic fibrosis transmembrane conductance regulator to promote development of pancreatitis. *Gastroenterology* **148**, 427-439.e16 (2015).
75. Huang, W. *et al.* Fatty acid ethyl ester synthase inhibition ameliorates ethanol-induced Ca2+-dependent mitochondrial dysfunction and acute pancreatitis. *Gut* **63**, 1313–1324 (2014).
76. Lewis, S. *et al.* Acute inhibition of PMCA4, but not global ablation, reduces blood pressure and arterial contractility via a nNOS-dependent mechanism. *J. Cell. Mol. Med.* **22**, 861–872 (2018).
77. Fanczal, J. *et al.* TRPM2-mediated extracellular Ca2+ entry promotes acinar cell necrosis in biliary acute pancreatitis. *J. Physiol.* **598**, 1253–1270 (2020).
78. Yokoyama, T., Takemoto, M., Hirakawa, M. & Saino, T. Different immunohistochemical localization for TMEM16A and CFTR in acinar and ductal cells of rat major salivary glands and exocrine pancreas. *Acta Histochem.* **121**, 50–55 (2019).
79. Go, C. K. *et al.* Ca2+ export pump PMCA clears near-membrane Ca2+ to facilitate store-operated Ca2+ entry and NFAT activation. *Sci. Signal.* **12**, eaaw2627 (2019).
80. Stafford, N., Wilson, C., Oceandy, D., Neyses, L. & Cartwright, E. J. The Plasma Membrane Calcium ATPases and Their Role as Major New Players in Human Disease. *Physiol. Rev.* **97**, 1089–1125 (2017).

81. Strubberg, A. M. *et al.* Cftr Modulates Wnt/β-Catenin Signaling and Stem Cell Proliferation in Murine Intestine. *Cell. Mol. Gastroenterol. Hepatol.* **5**, 253–271 (2018).
82. Mukherjee, R. *et al.* Mitochondrial injury in pancreatitis. *Cell Calcium* **44**, 14–23 (2008).
83. Billet, A. & Hanrahan, J. W. The secret life of CFTR as a calcium-activated chloride channel. *J. Physiol.* **591**, 5273–5278 (2013).
84. Park, S. *et al.* Irbit mediates synergy between ca(2+) and cAMP signaling pathways during epithelial transport in mice. *Gastroenterology* **145**, 232–241 (2013).
85. Antigny, F. *et al.* Dysfunction of mitochondria Ca2+ uptake in cystic fibrosis airway epithelial cells. *Mitochondrion* **9**, 232–241 (2009).
86. Antigny, F., Norez, C., Becq, F. & Vandebrouck, C. Calcium homeostasis is abnormal in cystic fibrosis airway epithelial cells but is normalized after rescue of F508del-CFTR. *Cell Calcium* **43**, 175–183 (2008).
87. Antigny, F. *et al.* Transient receptor potential canonical channel 6 links Ca2+ mishandling to cystic fibrosis transmembrane conductance regulator channel dysfunction in cystic fibrosis. *Am. J. Respir. Cell Mol. Biol.* **44**, 83–90 (2011).
88. Balghi, H. *et al.* Enhanced Ca2+ entry due to Orai1 plasma membrane insertion increases IL-8 secretion by cystic fibrosis airways. *FASEB J. Off. Publ. Fed. Am. Soc. Exp. Biol.* **25**, 4274–4291 (2011).
89. Maléth, J. & Hegyi, P. Calcium signaling in pancreatic ductal epithelial cells: an old friend and a nasty enemy. *Cell Calcium* **55**, 337–345 (2014).
90. Pallagi, P., Madácsy, T., Varga, Á. & Maléth, J. Intracellular Ca2+ Signalling in the Pathogenesis of Acute Pancreatitis: Recent Advances and Translational Perspectives. *Int. J. Mol. Sci.* **21**, (2020).
91. Maléth, J. *et al.* Non-conjugated chenodeoxycholate induces severe mitochondrial damage and inhibits bicarbonate transport in pancreatic duct cells. *Gut* **60**, 136–138 (2011).
92. Franca, A. *et al.* Effects of Endotoxin on Type 3 Inositol 1,4,5-Trisphosphate Receptor in Human Cholangiocytes. *Hepatol. Baltim. Md* **69**, 817–830 (2019).
93. Guerra, M. T. & Nathanson, M. H. Calcium signaling and secretion in cholangiocytes. *Pancreatol. Off. J. Int. Assoc. Pancreatol. IAP Al* **15**, S44-48 (2015).
94. Hegedűs, L. *et al.* Molecular Diversity of Plasma Membrane Ca2+ Transporting ATPases: Their Function Under Normal and Pathological Conditions. *Adv. Exp. Med. Biol.* **1131**, 93–129 (2020).
95. Criddle, D. N. *et al.* Fatty acid ethyl esters cause pancreatic calcium toxicity via inositol trisphosphate receptors and loss of ATP synthesis. *Gastroenterology* **130**, 781–793 (2006).
96. Petersen, O. H. *et al.* Fatty acids, alcohol and fatty acid ethyl esters: toxic Ca2+ signal generation and pancreatitis. *Cell Calcium* **45**, 634–642 (2009).
97. Tóth, E. *et al.* Novel mitochondrial transition pore inhibitor N-methyl-4-isoleucine cyclosporin is a new therapeutic option in acute pancreatitis. *J. Physiol.* **597**, 5879–5898 (2019).
98. Barry, P. J. *et al.* Triple Therapy for Cystic Fibrosis Phe508del-Gating and -Residual Function Genotypes. *N. Engl. J. Med.* **385**, 815–825 (2021).
99. Munce, D., Lim, M. & Akong, K. Persistent recovery of pancreatic function in patients with cystic fibrosis after ivacaftor. *Pediatr. Pulmonol.* **55**, 3381–3383 (2020).
100. Bruen, C. *et al.* Auxora for the Treatment of Patients With Acute Pancreatitis and Accompanying Systemic Inflammatory Response Syndrome: Clinical Development of a Calcium Release-Activated Calcium Channel Inhibitor. *Pancreas* **50**, 537–543 (2021).

101. Berrocal, M., Corbacho, I., Gutierrez-Merino, C. & Mata, A. M. Methylene blue activates the PMCA activity and cross-interacts with amyloid β-peptide, blocking Aβ-mediated PMCA inhibition. *Neuropharmacology* **139**, 163–172 (2018).
102. Pushparajah Mak, R. S. & Liebelt, E. L. Methylene Blue: An Antidote for Methemoglobinemia and Beyond. *Pediatr. Emerg. Care* **37**, 474–477 (2021).

Author names in bold designate shared co-first authorship.